



HAL
open science

Zermelo Navigation Problems on Surfaces of Revolution and Geometric Optimal Control

Bernard Bonnard, Olivier Cots, Boris Wembe

► **To cite this version:**

Bernard Bonnard, Olivier Cots, Boris Wembe. Zermelo Navigation Problems on Surfaces of Revolution and Geometric Optimal Control. ESAIM: Control, Optimisation and Calculus of Variations, 2023, 29 (60), pp.34. 10.1051/cocv/2023052 . hal-03209491v5

HAL Id: hal-03209491

<https://hal.science/hal-03209491v5>

Submitted on 4 Jul 2023

HAL is a multi-disciplinary open access archive for the deposit and dissemination of scientific research documents, whether they are published or not. The documents may come from teaching and research institutions in France or abroad, or from public or private research centers.

L'archive ouverte pluridisciplinaire **HAL**, est destinée au dépôt et à la diffusion de documents scientifiques de niveau recherche, publiés ou non, émanant des établissements d'enseignement et de recherche français ou étrangers, des laboratoires publics ou privés.

Zermelo navigation problems on surfaces of revolution and geometric optimal control

B. Bonnard*[†], O. Cots[‡], B Wembe[§]

01 July 2023

abstract. In this article, the historical study from Carathéodory-Zermelo about computing the quickest nautical path is generalized to Zermelo navigation problems on surfaces of revolution, in the frame of geometric optimal control. Using the Maximum Principle, we present two methods dedicated to analyzing the geodesic flow and to compute the conjugate and cut loci. We apply these calculations to investigate case studies related to applications in hydrodynamics, space mechanics and geometry.

résumé. Dans cet article, on généralise l'étude historique de Carathéodory-Zermelo sur le calcul du chemin nautique le plus rapide, aux problèmes de navigation de Zermelo sur des surfaces de révolution, dans le cadre du contrôle optimal géométrique. En utilisant le Principe du Maximum, on présente deux méthodes permettant d'analyser le flot géodésique et de calculer les lieux conjugués et de coupure en lien avec l'optimalité locale et globale des trajectoires. Ces calculs sont ensuite appliqués à des cas d'études liés à des applications en hydrodynamique, en mécanique spatiale et en géométrie.

Key words. Zermelo navigation problems, Optimal control, Abnormal geodesics, Conjugate and cut loci, Regularity of the value function.

1 Introduction

A Zermelo navigation problem on a surface of revolution M is defined by the pair (g, F_0) where g is the metric on M induced by the Euclidean metric of \mathbb{R}^3 and F_0 is a vector field on M called the current. Using the control formalism, see[16], the Zermelo navigation problem can be set as the *time minimal transfer* between two points q_0, q_1 for the control system:

$$\frac{dq(t)}{dt} = F_0(q(t)) + \sum_{i=1}^2 u_i(t)F_i(q(t)),$$

$u = (u_1, u_2)$, $\|u\| = \sqrt{u_1^2 + u_2^2} \leq 1$, where $q = (r, \theta)$ are the polar coordinates for the metric g which takes the form $g = dr^2 + m^2(r) d\theta^2$, see [6], the current F_0 being invariant by rotation and F_1, F_2 form an orthonormal frame. The surface M is split into rectangles $r_0 < r < r_1$ with *weak current* if $\|F_0\|_g < 1$ or *strong current* if $\|F_0\|_g > 1$. Such a problem is a generalization of the *historical problem of the quickest nautical path* analyzed by Carathéodory and Zermelo [18, 34], which have provided a complete study in the case of a linear current.

The first contribution of this article is to set the problem in the frame of geometric control, starting with the Maximum Principle [28] to introduce two different methods to analyze the geodesic flow. First of all, using the *heading angle* α of the ship, the system can be extended to an affine single input system:

$$\frac{d\tilde{q}(t)}{dt} = X(\tilde{q}(t)) + v(t)Y(\tilde{q}(t)), \quad (1)$$

*McTAO, INRIA Sophia Antipolis, Nice, France, bbonnard@u-bourgogne.fr

[†]Institut de Mathématiques de Bourgogne, UBFC, France,

[‡]ENSEEIH, IRIT, Toulouse, France, olivier.cots@irit.fr

[§]University of Paderborn, Germany, wboris@math.upb.de

with $\tilde{q} = (r, \theta, \alpha)$ and v is the time derivative of α . Such a transformation being called a *Carathéodory-Zermelo-Goh (CZG) transformation* in this article. Using this approach, geodesics correspond to the so-called *singular trajectories* associated to (1) with $v \in \mathbb{R}$, see [10] for this concept, and the geodesics can be classified into *normal* and *abnormal geodesics*, the second being on the zero level of the induced Hamiltonian. This approach allows to compute conjugate points along normal geodesics, where optimality is lost for the C^1 -topology on the set of geodesics that is in a conic neighborhood defined by the heading angle, this using the results and technical approach in [14], based on the computation of semi-normal forms. Furthermore, using similar techniques a first result of this article is to define and compute conjugate points along abnormal geodesics. More precisely, as already detected in the historical study, they correspond to a *cusp singularity* of the abnormal geodesics, when meeting the transition set $\|F_0\|_g = 1$ between the strong and weak currents.

The second main technical contribution of this article is (following the approach used by I. Kupka in SR-geometry [25]) to analyze the set of geodesics using a one-dimensional *mechanical system*, with an *extended potential* $V(r, p_\theta)$ where the r-dynamics takes the form:

$$\left(\frac{dr(t)}{dt}\right)^2 = 1 - V(r(t), p_\theta), \quad (2)$$

p_θ being the adjoint variable of θ which is constant using the Clairaut relation in the Hamiltonian frame. This leads to the analysis of the geodesic flow using an extension of the *Morse-Reeb classification* for 2d-Hamiltonian dynamics, see [6, p. 21], and in particular to provide a stratification of the set of geodesics into r-periodic or r-aperiodic curves (*i.e.* periodic or not with respect to the variable r). Also in this frame, complicated dynamics can occur, in particular related to the existence of *Reeb components* in the geodesic foliation of M , see [20, 22] for such occurrences in the modern study of foliation and dynamical systems.

Finally, the third contribution of this article is to use the above techniques to analyze in details *different case studies* which form the core of this article, motivated by geometry and control theory. In each case, our aim is to compute the time optimal synthesis in the sense of [30, 31] in an adapted rectangular domain R of the initial point q_0 . This means to compute in each case the *cut locus* $\Sigma(q_0)$, where optimality is lost along geodesics initiating from q_0 , when restricted to R . In particular, three cases are studied in details. The first case is to analyze the historical example in our frame. In this case, every geodesic is r-aperiodic and the cut locus contains a single branch of the abnormal geodesic, terminating with a cusp singularity, when meeting the set $\|F_0\|_g = 1$. The second case deals with the Riemannian metric on a two-sphere of revolution, which appears in space mechanics and was analyzed in full details in [7]. Introducing a small current corresponds to the Finsler case analyzed in [5] for which the properties of conjugate and cut loci are well known, thanks to the continuity of the value function, and it is similar to the Riemannian case [19, p. 267]. Moreover, the techniques of Poincaré and Myers can be used to compute the cut locus [27]. But we extend the analysis to the case of a strong current, and we show that the cut locus splits into two branches. This phenomenon is related to the optimality status of the abnormal geodesics [15] and to the shape of the small-time balls [12]. The third case study concerns the extension of the evolution of a passive tracer near a vortex and it was analyzed in details in [13]. This study motivated by applications in hydrodynamics [1] but also in relation with the N-body dynamics [26] is generalized and indicate the complexity of the geodesic dynamics, in relation with many Reeb components.

This article is organized as follows. In Section 2, we introduce the general concepts and definitions, and a large collection of case studies. In Section 3, we introduce the geometric tools of this article in relation with the geodesic curves, solution of the Maximum Principle. We define two different parameterizations of those curves. The first one is the CZG-extension related to conjugate points computations in both normal and abnormal cases and integration of the geodesic curves, using quadratures, in relation with Clairaut condition on surfaces of revolution. The second parameterization is described in Section 4 introducing the generalized potential and the generalized Morse-Reeb classification of the geodesics. In Section 5, which is the core of this article, we investigate in details the case studies. The final Section 6 is the conclusion which summarizes our contributions and proposes further studies.

2 Definitions, notations and the list of case studies

2.1 Definitions and notations

Let M be a smooth *surface of revolution* with g the induced Riemannian metric and let T^*M be the *cotangent bundle* endowed with the *Liouville canonical form* $\alpha = pdq$. We recall for Theorem 4.1 that a *Lagrangian manifold* is a 2d-submanifold where $d\alpha$ is zero. We denote by $q = (r, \theta)$ the *normal (polar) coordinates* on the *covering Riemannian manifold* M^c defined as $0 < r < \bar{r}$ and $\theta \in \mathbb{R}$ for a certain \bar{r} , cf. [9]. Considering these coordinates, the metric takes the form $g = dr^2 + m^2(r) d\theta^2$ setting $m(r) > 0$ and the vector fields $F_1 = \frac{\partial}{\partial r}$ and $F_2 = \frac{1}{m(r)} \frac{\partial}{\partial \theta}$ define the canonical *orthonormal frame*. The lines $r = \text{constant}$ are called the *parallels* and the lines $\theta = \text{constant}$ are called the *meridians*. A *Zermelo navigation problem of revolution* is defined by a triplet (M, g, F_0) where the vector field F_0 defining the current is invariant by θ -rotation, and we shall assume to cover the case studies that F_0 is oriented along the parallels only so that on M^c it can be written $F_0 = \mu(r) \frac{\partial}{\partial \theta}$. If $\mu(r)$ is constant (resp. linear) this is called the *constant* (resp. *linear*) *current case*. We define an *adapted neighborhood* of a point $q_0 \in M^c$ as a rectangle $R = [r_1, r_2] \times [\theta_1, \theta_2] \subset M^c$ containing q_0 .

From the control point of view, the Zermelo navigation problem can be written in q -coordinates as: minimize the transfer time between two points (q_0, q_1) for the system

$$\frac{dq(t)}{dt} = F_0(q(t)) + \sum_{i=1,2} u_i(t) F_i(q(t)),$$

with admissible controls in the set of measurable functions defined on $[0, +\infty)$ and valued in $\{u \mid \|u\| \leq 1\}$. The *heading angle* α of the ship in the canonical frame is defined by $u_1 = \sin \alpha$, $u_2 = \cos \alpha$, whenever $\|u\| = 1$, where according to Clairaut interpretation, α is the angle with respect to the parallel. Due to the symmetry of revolution, we can decompose the covering space into rectangles where we have either (at least in their interiors) a *weak current* if $\|F_0\|_g < 1$ or a *strong current* if $\|F_0\|_g > 1$, the transition between the two cases, when $\|F_0\|_g = 1$, being called the case of a *moderate current*. Furthermore, we can cover M^c by adapted neighborhoods on which we can restrict the dynamics. For such an adapted neighborhood denoted R and a fixed point $q_0 \in R$, the navigation problem is called *geodesically complete* on R from q_0 if for any q_1 in R , there exists a geodesic contained in R joining q_0 to q_1 . Besides, we denote by $q_1 \mapsto T(q_0, q_1)$ the *time minimal value function* representing the minimal transfer time from q_0 to q_1 .

2.2 List of motivating case studies

2.2.1 The historical example

A founding problem in classical calculus of variations is the problem called *quickest nautical path* introduced by Carathéodory and Zermelo [18, 34] for a ship navigating on a river and aiming to reach the opposite shore in minimum time. Hence, M is the 2d-Euclidean space with metric $g = dx^2 + dy^2$ in the coordinates $q = (x, y)$, y being the distance to the shore. To make a complete analysis, they have considered a *linear current* of the form $F_0 = y \frac{\partial}{\partial x}$. We shall refer to this case all along this article as the *historical example*. Using our notation to fix parallels and meridians, we must set $x = \theta$, $y = r$, so that the ambient manifold is the Euclidean space with metric $g = dr^2 + d\theta^2$ and $F_0 = r \frac{\partial}{\partial \theta}$.

2.2.2 The vortex case

This case was analyzed in [13] and will be generalized in our study. The ambient space is the punctured Euclidean space and the vortex is localized at the origin and the ship is a *passive tracer* in hydrodynamics whose motion is described by:

$$\frac{dx}{dt}(t) = -\frac{ky(t)}{x(t)^2 + y(t)^2} + u_1(t), \quad \frac{dy}{dt}(t) = +\frac{kx(t)}{x(t)^2 + y(t)^2} + u_2(t),$$

where $k > 0$ is the *circulation parameter*. The problem is written in polar coordinates $x = r \cos \theta$, $y = r \sin \theta$ so that the Euclidean metric takes the form $g = dr^2 + r^2 d\theta^2$ and the current becomes $F_0 = \frac{k}{r^2} \frac{\partial}{\partial \theta}$. The ambient manifold is defined by $r \geq 0$, F_0 having a pole at the vortex identified to $r = 0$.

2.2.3 The averaged Kepler case

The Riemannian problem related to the averaged Kepler problem in space mechanics (see [7]) can be extended to a metric on a two-sphere of revolution defined in normal coordinates by $m^2(r) = \frac{\cos^2 r}{1-\lambda \cos^2 r}$ where λ is a homotopic parameter, deforming the round sphere (for $\lambda = 0$) to the singular metric called the *Grushin case* (for $\lambda = 1$) and $\lambda = 4/5$ corresponds to the *averaged Kepler case*. For this case, we will consider a constant current on the covering space.

2.2.4 Ellipsoid of revolution

This standard problem of geometry is analyzed in [24]. The ellipsoid of revolution is generated by the curve: $y = \sin \varphi$, $z = \varepsilon \cos \varphi$ where $0 < \varepsilon < 1$ corresponds to the *oblate* (flattened) case while $\varepsilon > 1$ corresponds to the *prolate* (elongated) case. The metric takes the form $g = F_1(\varphi) d\varphi^2 + F_2(\varphi) d\theta^2$, with $F_1(\varphi) = \cos^2 \varphi + \varepsilon^2 \sin^2 \varphi$, $F_2 = \sin^2 \varphi$. The metric can be set in the polar form using a quadrature. This defines a family of metrics on a two-sphere of revolution, depending upon ε .

2.2.5 The Serret-Andoyer case

The Serret-Andoyer metric studied in [11] corresponds to a representation of a mechanical pendulum. It is given in the normal form by taking $m^2(r) = (A \operatorname{cn}^2(\alpha r, k) + B \operatorname{sn}^2(\alpha r, k))^{-1}$, where cn and sn are Jacobi elliptic functions so that $m(r)$ is periodic and moreover $m(r) = m(-r)$. we have $k^2 = \frac{B-A}{C-A}$, $\alpha = \sqrt{C-A}$, where $0 < A < B < C$ are parameters.

Remark 1. For the two last metrics, we can also define a Zermelo navigation problem by adding for instance a constant or a linear current on the covering space. We refer to [23], for the analysis of the ellipsoid of revolution in the Finslerian case. Note also that on a two-sphere of revolution a constant current corresponds to a linear rotation with the axis Oz .

3 The geometric tools from control theory and the Hamiltonian analysis

3.1 Generalities and the Maximum Principle

If not mentioned, all the objects are in a smooth category. Recall that we consider a Zermelo navigation problem of revolution determined by a triplet (M, g, F_0) . The vector field defining the current can be taken in the form $F_0 = \mu(r) \frac{\partial}{\partial \theta}$ which permit to cover all the cases defined above. The Zermelo navigation problem on the covering space M^c consists to a time minimal transfer between two points (q_0, q_1) for the control system:

$$\frac{dq(t)}{dt} = F_0(q(t)) + \sum_{i=1,2} u_i(t) F_i(q(t)), \quad (3)$$

with $u = (u_1, u_2)$, $\|u\| \leq 1$ and the set of admissible controls \mathcal{U} is the set of measurable mappings defined on $[0, +\infty)$ and valued in the domain $\mathbf{U} = \{u \mid \|u\| \leq 1\}$. Given $q_0 \in M^c$ and $u \in \mathcal{U}$ we denote by $q(\cdot, q_0, u)$ the solution of (3) with $q(0) = q_0$, and defined on a maximal interval J . We introduce the *pseudo-Hamiltonian* associated to the cost (extended) system

$$H(z, u) = H_0(z) + u_1 H_1(z) + u_2 H_2(z) + p^0$$

with $z = (q, p)$, $p = (p_r, p_\theta)$ being called the *adjoint vector*, $H_i(z) = p \cdot F_i(q)$ being, for $i = 0, 1, 2$, the Hamiltonian lift of the vector field F_i , where \cdot denotes the standard inner product, and finally p^0 is a constant representing the dual variable of the cost. We define the *maximized* (or true) *Hamiltonian* by the maximization condition:

$$\mathbf{H}(z) = \max_{\|u\| \leq 1} H(z, u).$$

Let $q_0 \in M^c$ and (t_f, u) an optimal solution of the Zermelo navigation problem with $q(\cdot) = q(\cdot, q_0, u)$ the associated optimal trajectory. According to the Pontryagin's Maximum Principle [28], there exists an absolutely

continuous function p and a scalar $p^0 \leq 0$ such that the 4-uplet (q, p, u, p^0) satisfies, for almost every $t \in [0, t_f]$, the following conditions:

$$\begin{aligned} \dot{q}(t) &= \nabla_p H(q(t), p(t), u(t)), & \dot{p}(t) &= -\nabla_q H(q(t), p(t), u(t)), \\ \mathbf{H}(q(t), p(t)) &= H(q(t), p(t), u(t)) = \max_{w \in \mathbf{U}} H(q(t), p(t), w) = 0, \end{aligned} \quad (4)$$

the pair $(p(\cdot), p^0)$ never vanishes.

Definition 3.1. An extremal is a solution $z(\cdot) = (q(\cdot), p(\cdot))$ of (4) and a projection of an extremal is called a geodesic. It is called strict if p is unique up to a factor, normal if $p^0 \neq 0$ and abnormal (or exceptional) if $p^0 = 0$. In the normal case it is called hyperbolic (resp. elliptic) if $p^0 < 0$ (resp. $p^0 > 0$).

Since F_1 and F_2 form a frame, then the following will hold in our case.

Proposition 3.1. The trajectory $q(\cdot)$ is the projection of the extremal $z(\cdot) = (q(\cdot), p(\cdot))$, solution of the system

$$\dot{z}(t) = \vec{\mathbf{H}}(z(t)) \quad (5)$$

where the Hamiltonian vector field $\vec{\mathbf{H}}$ is given by $\vec{\mathbf{H}} = (\nabla_p \mathbf{H}, -\nabla_q \mathbf{H})$. Besides, the optimal control is given in feedback form by

$$u_i(z) = \frac{H_i(z)}{\|p\|_g}, \quad i = 1, 2, \quad (6)$$

and the maximized Hamiltonian reads $\mathbf{H}(z) = H_0(z) + \|p\|_g + p^0$, setting $\|p\|_g = \sqrt{H_1^2(z) + H_2^2(z)}$.

Introducing the following definition, we can use results from [10, Chap. 3] to characterize normal and abnormal extremals.

Definition 3.2. The fixed time extremity mapping is the map $E^{q_0, t_f} : u \mapsto q(t_f, q_0, u)$ and the extremity mapping is the map $E^{q_0} : u \mapsto q(\cdot, q_0, u)$, the set of inputs u being defined on a subdomain of L^∞ , endowed with the L^∞ -norm topology. The accessibility set in time t_f , denoted $A(q_0, t_f)$, is the image of E^{q_0, t_f} and the accessibility set $A(q_0) = \bigcup_{t_f \geq 0} A(q_0, t_f)$ is the image of the extremity mapping.

Proposition 3.2. Take a reference extremal $z(\cdot) = (q(\cdot), p(\cdot))$ on $[0, t_f]$ where the corresponding control is given by (6). If we endow the set of controls valued in $\|u\| = 1$ with the L^∞ -norm topology we have:

1. In the normal case, $u(\cdot)$ is a singularity of the fixed time extremity mapping.
2. In the abnormal case, $u(\cdot)$ is a singularity of the extremity mapping.

Definition 3.3. Let $t \mapsto q(t)$ be a response of (3). It is called regular if it is a one-to-one immersion. From the Maximum Principle, the geodesics can be parameterized by the initial heading angle α_0 and fixing $q(0) = q_0$, we can define the exponential mapping as the map $\exp_{q_0} : (\alpha_0, t) \mapsto \Pi(\exp(t\vec{\mathbf{H}})(q_0, p_0(\alpha_0)))$ where Π is the q -projection: $(q, p) \mapsto q$. The cut point along a given geodesic is the first point where it ceases to be optimal and they will form the cut locus $\Sigma(q_0)$. The separating line $L(q_0)$ is the set of points where two minimizing geodesics starting from q_0 are intersecting.

3.2 Carathéodory-Zermelo-Goh transformation and integration of the geodesics

3.2.1 Carathéodory-Zermelo-Goh transformation

In the historical example, Carathéodory-Zermelo integrated the dynamics using the heading angle α to parameterize the geodesics, see [16, p. 77]. This corresponds to the Goh transformation in optimal control, see [10, p. 98]. Next, we use this crucial point to make computations in the Lie algebraic frame and to relate the analysis of the navigation problem to the general study of [14].

Definition 3.4. Let us consider the control system (3) with the restriction $\|u\| = 1$. Then, we can set $u = (\cos \alpha, \sin \alpha)$, α being the heading angle of the ship. We denote by $\tilde{q} = (q, \alpha)$ the extended state and we

introduce the vector fields $X(\tilde{q}) = F_0(q) + \cos \alpha F_1(q) + \sin \alpha F_2(q)$ and $Y(\tilde{q}) = \frac{\partial}{\partial \alpha}$. This leads us to prolongate (3) into the single-input affine system:

$$\frac{d\tilde{q}}{dt}(t) = X(\tilde{q}(t)) + v(t)Y(\tilde{q}(t)) \quad (7)$$

and the derivative of the heading angle $v(t) = \frac{d\alpha}{dt}(t)$ is called the accessory control. Denoting $\tilde{z} = (\tilde{q}, \tilde{p}) = ((q, \alpha), (p, p_\alpha))$, this leads to define the extended pseudo-Hamiltonian

$$\tilde{H}(\tilde{z}, v) = \tilde{p} \cdot (X(\tilde{q}) + vY(\tilde{q})) + p^0. \quad (8)$$

Parameterization of the geodesic curves in this extension. From [10, Chap. 6], in this representation, geodesic curves extend to singular trajectories of (7), where the accessory control v belongs to the whole set \mathbb{R} .

Definition 3.5. The Lie bracket of two vector fields U, V is computed with the convention

$$[U, V](\tilde{q}) = \frac{\partial U}{\partial \tilde{q}}(\tilde{q})V(\tilde{q}) - \frac{\partial V}{\partial \tilde{q}}(\tilde{q})U(\tilde{q})$$

and is related to the Poisson bracket $\{H_U, H_V\}(\tilde{z}) = dH_U(\tilde{z}) \cdot \overrightarrow{H}_V(\tilde{z})$ by the relation

$$\{H_U, H_V\}(\tilde{z}) = \tilde{p} \cdot [U, V](\tilde{q}),$$

where H_U and H_V are the Hamiltonian lifts of U and V .

Lemma 3.1. One has the following:

$$\begin{aligned} \frac{d}{dt} \frac{\partial \tilde{H}}{\partial v} \Big|_{(\tilde{q}, \tilde{p}, v)} &= \tilde{p} \cdot [Y, X](\tilde{q}), \\ \frac{\partial}{\partial v} \frac{d^2}{dt^2} \frac{\partial \tilde{H}}{\partial v} \Big|_{(\tilde{q}, \tilde{p}, v)} &= \tilde{p} \cdot [[Y, X], Y](\tilde{q}) = \frac{\partial^2 H}{\partial \alpha^2} \Big|_{(q, p, u)}. \end{aligned}$$

Proposition 3.3. Let us introduce the following determinants:

$$D = \det(Y, [Y, X], [[Y, X], Y]), \quad D' = \det(Y, [Y, X], [[Y, X], X]), \quad D'' = \det(Y, [Y, X], X).$$

Assume that $D(\tilde{q})$ is not vanishing, then the singular control $v(\cdot)$ associated to the geodesics is given by the feedback

$$v(t) = v_s(\tilde{q}(t)) = -\frac{D'(\tilde{q}(t))}{D(\tilde{q}(t))} \quad (9)$$

and the geodesics extend to smooth solutions of

$$\frac{d\tilde{q}}{dt}(t) = X(\tilde{q}(t)) + v_s(\tilde{q}(t))Y(\tilde{q}(t)).$$

For this dynamics, one has:

- hyperbolic geodesics are in $DD'' > 0$,
- elliptic geodesics are in $DD'' < 0$,
- abnormal (or exceptional) geodesics are located in $D'' = 0$.

Proof. From [10, Sec. 3.4], taking a singular control-trajectory pair $(\tilde{q}(\cdot), v(\cdot))$, denoting $\tilde{z} = (\tilde{q}, \tilde{p})$ one has

$$\begin{aligned} H_Y(\tilde{z}) &= \{H_Y, H_X\}(\tilde{z}) = 0, \\ \{\{H_Y, H_X\}, H_X\}(\tilde{z}) + v \{\{H_Y, H_X\}, H_Y\}(\tilde{z}) &= 0 \end{aligned} \quad (10)$$

and this leads to

$$\begin{aligned} 0 &= \tilde{p} \cdot Y(\tilde{q}) = p_\alpha, \\ 0 &= \tilde{p} \cdot [Y, X](\tilde{q}), \\ 0 &= \tilde{p} \cdot ([Y, X], X](\tilde{q}) + v [[Y, X], Y](\tilde{q}). \end{aligned} \tag{11}$$

Hence, since $\tilde{p} \in \mathbb{R}^3 \setminus \{0\}$, \tilde{p} can be eliminated using (11) and the singular control reads as the singular feedback

$$v(t) = v_s(\tilde{q}(t)) = -\frac{D'(\tilde{q}(t))}{D(\tilde{q}(t))}.$$

Since $D(\tilde{q})$ is never vanishing, one has that $Y(\tilde{q})$, $[Y, X](\tilde{q})$ are linearly independent and the adjoint vector \tilde{p} is unique up to a factor. Thus, every geodesic is strict.

Moreover, the following condition called the strict *generalized* Legendre-Clebsch condition is satisfied:

$$\frac{\partial}{\partial v} \frac{d^2}{dt^2} \frac{\partial \tilde{H}}{\partial v} \Big|_{(\tilde{z}, v)} = \tilde{p} \cdot [[Y, X], Y](\tilde{q}) \neq 0$$

along any geodesic extension. This amounts to the strict Legendre-Clebsch condition: $\frac{\partial^2 \mathbf{H}}{\partial \alpha^2} \neq 0$.

The classification of the geodesics (in the strict case) into hyperbolic, elliptic and abnormal geodesics defines for the extension, the set $DD'' > 0$, $DD'' < 0$ and $D'' = 0$. \square

Proposition 3.4. *The dynamics of the geodesics in polar coordinates is given by:*

$$\dot{r} = \cos \alpha, \quad \dot{\theta} = \mu(r) + \frac{\sin \alpha}{m(r)}, \quad \dot{\alpha} = \mu'(r)m(r) \sin^2 \alpha - \frac{m'(r) \sin \alpha}{m(r)}. \tag{12}$$

Hence, the Hamiltonian geodesic flow is Liouville integrable [2, p. 269] with two involutive first integrals \mathbf{H} and p_θ .

Proof. Computing with polar coordinates $\tilde{q} = (r, \theta, \alpha)$ one has:

$$\begin{aligned} X &= \cos \alpha \frac{\partial}{\partial r} + \left(\mu(r) + \frac{\sin \alpha}{m(r)} \right) \frac{\partial}{\partial \theta} \\ Y &= \frac{\partial}{\partial \alpha} \end{aligned}$$

and Lie brackets computations give:

$$\begin{aligned} [Y, X](\tilde{q}) &= \sin \alpha \frac{\partial}{\partial r} - \frac{\cos \alpha}{m(r)} \frac{\partial}{\partial \theta}, \\ [[Y, X], Y](\tilde{q}) &= \cos \alpha \frac{\partial}{\partial r} + \frac{\sin \alpha}{m(r)} \frac{\partial}{\partial \theta}, \\ [[Y, X], X](\tilde{q}) &= \left(-\mu'(r) \sin \alpha + \frac{m'(r)}{m^2(r)} \right) \frac{\partial}{\partial \theta}. \end{aligned}$$

This leads to:

$$D(\tilde{q}) = \frac{1}{m(r)}, \quad D'(\tilde{q}) = -\mu'(r) \sin^2 \alpha + \frac{m'(r) \sin \alpha}{m^2(r)}, \quad D''(\tilde{q}) = \mu(r) \sin \alpha + \frac{1}{m(r)}.$$

Then, (12) follows from (9). On the other hand, the pseudo-Hamiltonian in the \tilde{q} -representation takes the form

$$H = p_r \cos \alpha + p_\theta \left(\mu(r) + \frac{\sin \alpha}{m(r)} \right) + p^0$$

and from the maximization condition with $v \in \mathbb{R}$, one has $\frac{\partial H}{\partial \alpha} = 0$. This gives the *Clairaut relation* $p_r \sin \alpha = \frac{p_\theta}{m(r)} \cos \alpha$. Assuming $p_\theta \neq 0$, then we have $\sin \alpha \neq 0$ and then plugging such p_r into H , we obtain the relation

$$p_\theta \left(\mu(r) + \frac{1}{m(r) \sin \alpha} \right) + p^0 = 0. \tag{13}$$

relating r to α and this leads to the parameterization of the geodesics solution of (12). The case $p_\theta = 0$ is clear since in this case, $\sin \alpha = 0$ and so $\dot{\alpha} = 0$. \square

Application to the historical example.

Proposition 3.5. *Let (x_0, y_0, γ_0) be the initial condition, where $\gamma = \pi/2 - \alpha$. The corresponding solution $(x(t), y(t), \gamma(t))$ is given as follows.*

- For $\gamma_0 = \pm\pi/2$ we have:

$$\gamma(t) = \gamma_0, \quad y(t) = \pm t + y_0 \quad \text{and} \quad x(t) = \pm \frac{t^2}{2} + y_0 t + x_0.$$

- For $\gamma_0 \in (-\pi/2, \pi/2)$, we have:

$$\begin{aligned} \gamma(t) &= \operatorname{atan}(\tan \gamma_0 - t), \quad y(t) = y_0 + \frac{1}{\cos \gamma_0} - \frac{1}{\cos \gamma(t)}, \\ x(t) &= \frac{1}{2} \left[\ln \left| \frac{\cos \gamma}{1 + \sin \gamma} \right| \right]_{\gamma_0}^{\gamma(t)} + \frac{1}{2} \left[\frac{\sin \gamma}{\cos^2 \gamma} \right]_{\gamma_0}^{\gamma(t)} + \left(y_0 + \frac{1}{\cos \gamma_0} \right) t + x_0. \end{aligned}$$

- For $\gamma_0 \in (-\pi, -\pi/2) \cup (\pi/2, \pi]$, we have:

$$\begin{aligned} \gamma(t) &= \pi + \operatorname{atan}(\tan \gamma_0 - t), \quad y(t) = y_0 + \frac{1}{\cos \gamma_0} - \frac{1}{\cos \gamma(t)}, \\ x(t) &= \frac{1}{2} \left[\ln \left| \frac{\cos \gamma}{1 + \sin \gamma} \right| \right]_{\gamma_0}^{\gamma(t)} + \frac{1}{2} \left[\frac{\sin \gamma}{\cos^2 \gamma} \right]_{\gamma_0}^{\gamma(t)} + \left(y_0 + \frac{1}{\cos \gamma_0} \right) t + x_0. \end{aligned}$$

The geodesics split (see Fig. 1) into hyperbolic, elliptic and abnormal geodesics, using respectively the conditions $DD'' > 0$, $DD'' < 0$ and $D'' = 0$.

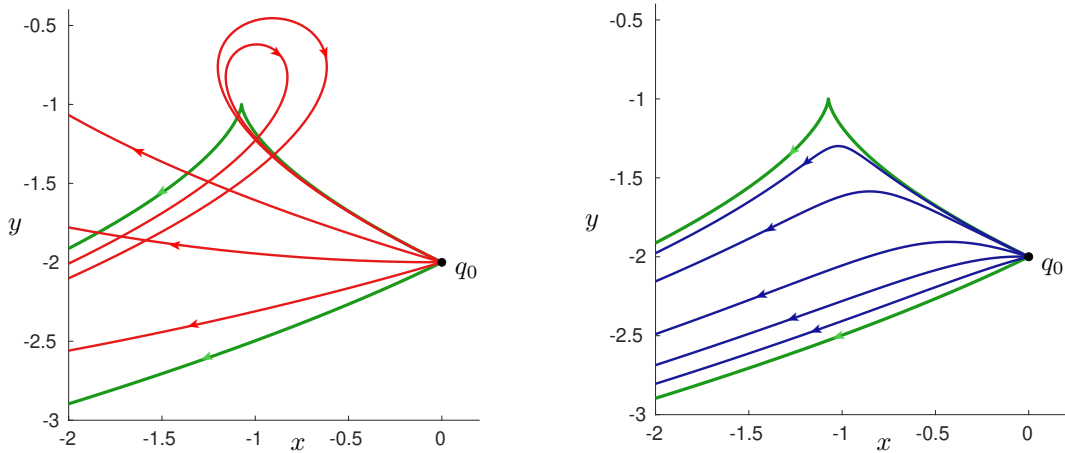


Figure 1: (Historical example) Geodesic flow in the hyperbolic (left) and elliptic (right) cases, in the whole conic neighborhood delimited by the two abnormal geodesics. The hyperbolic, elliptic and abnormal geodesics are represented resp. in red, blue and green. The initial point is $q_0 = (0, -2)$.

3.2.2 Moderate current domain and regularity properties of the geodesic curves

By definition in polar coordinates, the moderate current domain $\|F_0(q)\|_g = 1$ is given by the relation:

$$\mu^2(r) m^2(r) = 1$$

and so one can compute the decomposition of the domain into weak and strong current domains using the graph of the function $f(r) = \mu^2(r) m^2(r)$.

Definition 3.6. *Weak and strong current domains are defined respectively by: $f(r) < 1$ and $f(r) > 1$. A moderate parallel r_0 solution of $f(r) = 1$ is called regular if the intersection of the line $L(r) = 1$ with the graph of f is transversal at r_0 , i.e. the root r_0 is simple, so that at r_0 the moderate parallel defines a non-empty transition between weak and strong current domains.*

Lemma 3.2. *Let $\tilde{\sigma} = (q, \alpha)$ be a reference geodesic solution of (12) on $[0, t_f]$ and intersecting at time t_f the moderate current domain. Then:*

1. $\tilde{\sigma}$ is either hyperbolic or abnormal.
2. If $t \mapsto \tilde{\sigma}(t)$ is hyperbolic, then, $t \mapsto q(t)$ is an immersion on $[0, t_f]$, that is $\dot{q}(t)$ is non zero.
3. If $\tilde{\sigma}$ is abnormal, then, $t \mapsto \tilde{\sigma}(t)$ is an immersion on $(0, t_f)$ but $\dot{q}(t_f) = 0$.

Proof. Elliptic geodesics are contained in the strong current domain and only hyperbolic and abnormal geodesics can intersect the moderate current domain $\|F_0(q)\|_g = f(r) = 1$. Take a point $q = (r, \theta)$ in the moderate current domain. Then, there exist a heading angle α such that the following holds:

$$F_0(q) + \cos \alpha F_1(q) + \sin \alpha F_2(q) = 0. \quad (14)$$

From (12), this leads to the following relations for the dynamics:

$$\dot{r} = \cos \alpha = 0, \quad \dot{\theta} = \mu(r) + \frac{\sin \alpha}{m(r)} = 0. \quad (15)$$

Hence we obtain:

$$\alpha = \frac{\pi}{2} + k\pi, \quad \mu(r) \pm \frac{1}{m(r)} = 0.$$

Since $\dot{r} = \dot{\theta} = 0$, the geodesic intersecting the moderate current domain with the heading angle $\frac{\pi}{2} + k\pi$ is abnormal. In hyperbolic case, one has $\dot{q}(t_f) \neq 0$. The lemma is proved. \square

3.3 Computation of conjugate points using the CZG-transformation

The aim of this section is to provide algorithms to compute conjugate points. The *regular case* is covered in [14] whereas the recent article [15] analyzes in a general framework conjugate points along non-immersed abnormal geodesics in Zermelo navigation problems. Note that in both cases, the integrability property of the geodesic flow is not required, but *in fine* the semi-normal form is integrable cf. [14].

Definition 3.7. *Let $\tilde{\sigma}$ be a reference geodesic curve defined on $[0, t_f]$, $\tilde{\sigma}(t) = (q(t), \alpha(t))$, $\tilde{\sigma}(0) = (q_0, \alpha_0)$, with q_0 a fixed initial point. The first conjugate time along $\tilde{\sigma}$ is the first time t_{1c} such that $\tilde{\sigma}$ ceases to be minimizing for $t > t_{1c}$, with respect to geodesic curves $\tilde{q}(\cdot)$, with $\tilde{q}(0) = (q_0, \tilde{\alpha}_0)$, $|\alpha_0 - \tilde{\alpha}_0|$ small enough, that is in a conic neighborhood of the reference geodesic.*

First of all, we shall analyze the case where $\tilde{\sigma}(t)$ is a *regular geodesic*. It is based on [14].

3.3.1 A brief recap of [14] to determine conjugate points in the regular case

Semi-normal forms. We assume that the reference geodesic curve $t \mapsto \tilde{\sigma}(t)$ on $[0, t_f]$ is a one-to-one immersion. In this case, we can choose coordinates and a feedback so that $\tilde{\sigma} : t \rightarrow (t, 0, 0)$ and it can be taken as the response of the control $v = 0$. Further normalizations are obtained in the jet-spaces of (X, Y) in the neighborhood of $\tilde{\sigma}$.

Normal case. We can choose coordinates $\tilde{q} = (q_1, q_2, q_3)$ such that the system takes the form:

$$\begin{aligned} X &= \left(1 + \sum_{i,j=2}^3 a_{ij}(q_1) q_i q_j \right) \frac{\partial}{\partial q_1} + q_3 \frac{\partial}{\partial q_2} + \varepsilon_1(q), \\ Y &= \frac{\partial}{\partial q_3}, \end{aligned} \quad (16)$$

where $\varepsilon_1(q)$ can be neglected in the analysis and with $a_{33} < 0$ (resp. $a_{33} > 0$) in the hyperbolic (resp. elliptic) case.

Abnormal case. We can choose coordinates $\tilde{q} = (q_1, q_2, q_3)$ such that the system takes the form:

$$\begin{aligned} X &= (1 + q_2) \frac{\partial}{\partial q_1} + \frac{1}{2} a(q_1) q_2^2 \frac{\partial}{\partial q_3} + \varepsilon_2(q), \\ Y &= \frac{\partial}{\partial q_2}, \end{aligned} \tag{17}$$

where $\varepsilon_2(q)$ can be neglected in the analysis and where a is strictly positive.

See [14] for details about the computations and the descriptions of the mappings $q \mapsto \varepsilon_1(q), \varepsilon_2(q)$. In both cases, since $q_1(t) = t$ along the reference geodesic σ , one can replace q_1 by t in the semi-normal form (restricting our analysis to a conic neighborhood) and this allows to evaluate the accessibility set and its boundary. Hence, computing conjugate points to deduce the optimality status of the reference geodesic.

Definition 3.8. *The Jacobi (or variational) equation along the reference geodesic $\tilde{\sigma}$ is the equation:*

$$\dot{\delta\tilde{q}}(t) = \frac{\partial X_s}{\partial \tilde{q}}(\tilde{\sigma}(t)) \delta\tilde{q}(t) \tag{18}$$

with $X_s = X + v_s Y$ and v_s given by (9). A Jacobi field $J(t)$ is a solution of (18) which is said semi-vertical at $t = 0$ if $J(0) \in \mathbb{R}Y(\tilde{\sigma}(0))$.

From [14], one deduces the following.

Proposition 3.6.

1. *In the normal case, if t_c is a conjugate time, then, there exists a non-trivial Jacobi field J semi-vertical at $t = 0$ such that*

$$\det(J(t_c), Y(\tilde{\sigma}(t_c)), X(\tilde{\sigma}(t_c))) = 0.$$

Let t_{1c} be the first conjugate time, then, if the geodesic is hyperbolic (resp. elliptic) it is time minimizing (resp. maximizing) with respect to all geodesics in a conic neighborhood of the reference geodesic σ , up to time t_{1c} .

2. *In the abnormal case, the reference geodesic is both minimizing and maximizing in a conic neighborhood of $\tilde{\sigma}$.*

Remark 2. *The result is clear in the abnormal case due to (17), since $q_3(\cdot)$ is strictly positive, unless the geodesic curve is the reference geodesic. It was already observed by Carathéodory and Zermelo, see [18] where the abnormal geodesic are called "limit curves".*

The concept of generalized curvature using CZG-transformation in the normal case. It was defined in [10, p. 163] and it can be used in our Zermelo problem. The Jacobi equation along $\tilde{\sigma} : t \mapsto (t, 0, 0)$ takes the form:

$$\delta\ddot{y}(t) + \frac{\dot{a}(t)}{a(t)} \delta\dot{y}(t) + \frac{\dot{b}(t) - c(t)}{a(t)} \delta y(t) = 0 \tag{19}$$

where $a(t), b(t), c(t)$ denote in short the coefficients of $a_{33}, a_{23} + a_{32}, a_{22}$ in formula (16). The existence of conjugate time t_{1c} means that there exists a non-trivial solution of (19) satisfying $\delta y(0) = \delta y(t_{1c}) = 0$. It can be written in the normal form

$$\ddot{x}(t) + K(t)x(t) = 0 \tag{20}$$

setting $\delta y(t) = C(t)x(t)$ where

$$C(t) = \exp\left(\int_0^t -\frac{A(s)}{2} ds\right) = -\frac{1}{\sqrt{a(t)}}, \quad A(t) = \frac{\dot{a}(t)}{a(t)}$$

and $K(t)$ is the *generalized curvature* defined by

$$K(t) = C^{-1}(t)(\ddot{C}(t) + A(t)\dot{C}(t) + B(t)C(t)) \tag{21}$$

where $B(t) = \frac{\dot{b}(t) - c(t)}{a(t)}$.

Remark 3. Note that the generalized curvature depends upon the reference geodesic parameterization contrary to the Gauss curvature in Riemannian geometry. In Section 5, the averaged Kepler case will exhibit some geodesic images such that each of them is parameterized by an hyperbolic trajectory and an elliptic trajectory (for instance the equator).

3.3.2 Cusp singularity associated to a conjugate point in the non-regular (abnormal) case

Next, we use [15] to describe the cusp singularity of the abnormal geodesics when meeting the transition between the strong and weak current domains. It is based on [32] in the algebraic case and [3] in the C^∞ -case. Let $\gamma: t \mapsto (x(t), y(t))$ be a planar smooth curve. We recall that if a point $\gamma(t_{\text{cusp}})$ is a cusp point of order (p, q) , $2 \leq p \leq q$, then $\gamma^{(p)}(t_{\text{cusp}})$ and $\gamma^{(q)}(t_{\text{cusp}})$ are independent. It is called an *ordinary* (or a *semicubical*) *cusp point* if it is a cusp point of order (p, q) with $p = 2$ and $q = 3$. From [32, p. 56], an algebraic model in $\mathbb{R}[x, y]$ at an ordinary cusp $\gamma(t_{\text{cusp}})$ is given by the equation $x^3 - y^2 = 0$. Moreover it is the transition between a \mathbb{R} -node solution of the equation $x^3 - x^2 + y^2 = 0$, where the origin is a double point with two distinct tangents at 0: $x \pm y = 0$ and a \mathbb{C} -node solution of $x^3 + x^2 + y^2 = 0$ with two complex tangents at 0 given by $x \pm iy = 0$ and with two distinct components $x = y = 0$ and a smooth real branch (see also [15] for more details and Fig. 2 for an illustration).

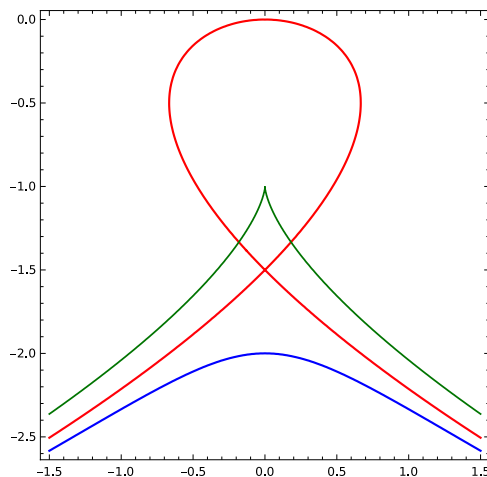


Figure 2: Miniversal unfolding of the cusp singularity in the quickest nautical path and with fixed horizontal symmetry in an adapted neighborhood. Red, green and blue respectively correspond to $y < -1, = 0, > -1$.

A neat description from singularity theory suitable in our analysis is given by [3, p. 65] and is associated to a typical perestroika of a plane curve depending on a parameter and having a semicubical cusp point for some value of the parameters, where the curves sweep an umbrella while their inflectional tangents sweep another umbrella surface. Below, we give some results to describe the properties of semicubical cusp points in relation with abnormal geodesics as well as the optimality of abnormal and hyperbolic geodesics in the neighborhood of cusp points.

Proposition 3.7. Consider a reference abnormal geodesic $\tilde{\sigma}_a = (\sigma_a, \alpha_a)$ defined on $[t_1, t_2]$, $t_1 < 0 < t_2$ so that at $t = 0$, σ_a meets a regular moderate parallel r_0 at $q_1 = \sigma_a(0)$. Denote $\sigma(t_1) = q_0$ and assume that $\dot{\alpha}_a(0) \neq 0$. Then, there exists a neighborhood V of q_1 such that for every geodesic starting from q_0 one has:

1. The abnormal geodesic σ_a meets the boundary at a semicubical cusp with a vertical tangent.
2. Hyperbolic geodesics are self-intersecting curves corresponding to a \mathbb{R} -node.
3. elliptic geodesics exist only in the strong current domain and correspond to a \mathbb{C} -node.

Proof. The proof follows from [15] and is illustrated by Fig. 3. □

Theorem 3.1. Under the previous assumptions, there exists a neighborhood V of q_1 , a point q_0 in $V \cap \sigma_a(\cdot)$ in which we have:

1. The abnormal arc is optimal from q_0 up to the cusp point q_1 included which corresponds to a conjugate point in the abnormal case.
2. Self-intersecting geodesics starting from q_0 are optimal up to their intersection point q_2 with the abnormal arc, the point q_2 being excluded. Hence, q_2 corresponds to a cut point.
3. The time minimal value function $T: q_2 \mapsto T(q_0, q_2)$ is discontinuous for each $q_2 \neq q_1$ on the abnormal geodesic.

Proof. The proof follows from [15] and is illustrated by Fig. 3. See also the cut loci of Fig. 4 for an illustration. \square

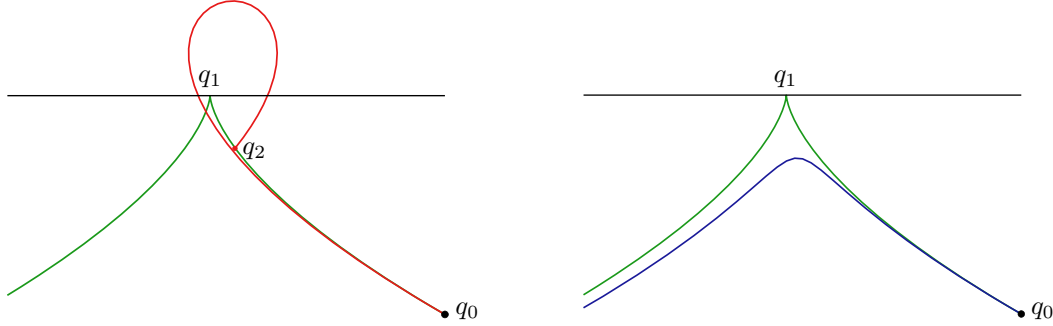


Figure 3: Unfolding of the cusp singularity depending upon the heading angle in an adapted neighborhood. (Left) Hyperbolic geodesics in a conic neighborhood with a self-intersection. (Right) Elliptic geodesics. The abnormal arc $\widehat{q_0q_1}$ is the limit curve already observed by Carathéodory.

Corollary 3.1. *Under the previous assumptions, the abnormal arc σ_a is optimal in the whole domain of strong current up to r_0 , restricting to a conic neighborhood.*

Proof. Let $\tilde{\sigma}_a: t \mapsto \tilde{\sigma}_a(t) = (\sigma_a(t), \alpha_a(t))$, $t \in [t_1, 0]$, $t_1 < 0$ (where $-t_1$ not necessarily small) be the reference abnormal geodesic. From the previous theorem, the abnormal arc starting from $q_2 = \sigma_a(t_2)$ with $t_1 < t_2 < 0$, t_2 small enough, is optimal from q_2 to q_1 . Moreover, the abnormal arc from $q_0 = \sigma(t_1)$ corresponds to an immersed curve and thus from [14], it is optimal on the whole strong current domain, restricting to a conic neighborhood. Hence, concatenating the two arcs allows us to conclude. \square

3.3.3 Time minimal synthesis in the historical example in an adapted rectangle

In this section we use the global parameterization of the geodesic curves given by Proposition 3.4 to compute the time minimal synthesis in an adapted rectangle containing the limit loop starting from q_0 . The limit loop starting from q_0 , see Fig. 4 for an illustration, is the geodesic starting from q_0 which returns to q_0 in minimum (positive) time. In the historical example, starting from q_0 in the strong current domain, there exists a limit loop denoted $l_{\text{loop}}(q_0)$ with return time denoted t_0 . The time minimal synthesis is represented on Fig. 4 and the main properties are the following.

Proposition 3.8. *In the historical example, taking a point q_0 in the strong current domain, then we can choose an adapted rectangle R containing the limit loop $l_{\text{loop}}(q_0)$ such that:*

1. $A(q_0, t_f)$ is a neighborhood of q_0 for $t_f > t_0$.
2. In the domain, the cut locus contains the whole branch of the abnormal geodesic arc $\widehat{q_0q_1}$ and is the union of the separating line $L(q_0)$ where abnormal and normal minimizing arcs intersect with unequal time and the terminating point q_1 which is a conjugate point of the non-immersed abnormal arc.

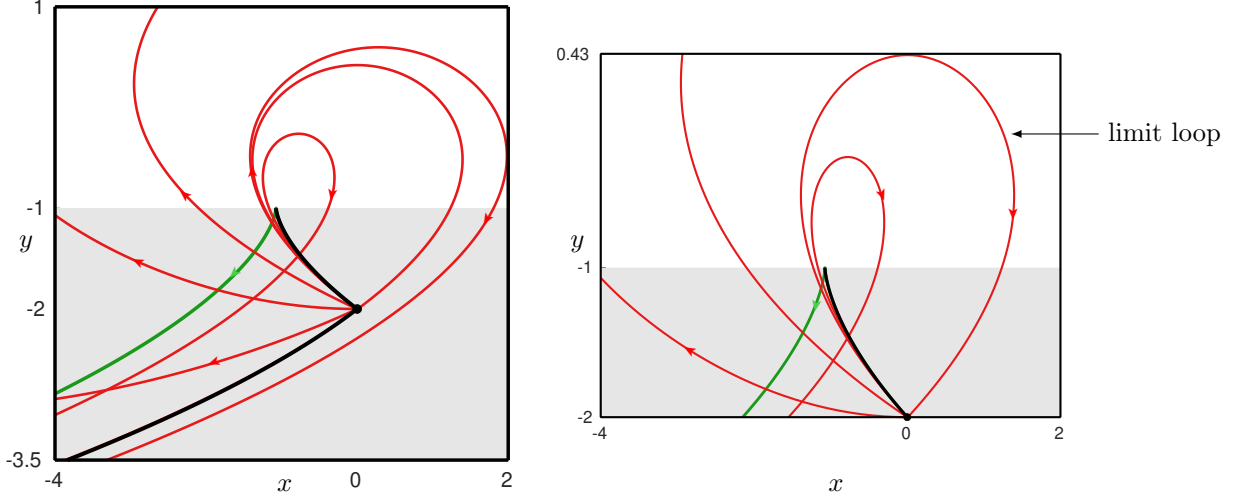


Figure 4: Time minimal synthesis in two different adapted rectangles containing the limit loop $l_{\text{loop}}(q_0)$. The second rectangle being delimited by the limit loop to emphasize the dependence of the cut locus to the considered adapted rectangle. In both cases, the cut locus (in black) contains the whole abnormal arc terminating at the cusp singularity. In gray is represented the strong current domain. The red curves are hyperbolic geodesics while the green represent abnormal.

4 Mechanical system and generalized Morse-Reeb classification

4.1 Mechanical representation in the Riemannian averaged Kepler case [7, 8]

In this section, we give a brief description of the mechanical representation in the Riemannian case, following the example of the averaged Kepler metric. In the Riemannian setting, roughly speaking, the time and energy minimization problems are equivalent. Classically, the (maximized) Hamiltonian associated to the energy minimization problem is preferred. This Hamiltonian is given by

$$\mathbf{H} = \frac{1}{2} \left(p_r^2 + \frac{p_\theta^2}{m^2(r)} \right) + p^0,$$

where the ambient manifold M is the (compact) 2-dimensional sphere of revolution and the metric g on the covering space M^c is given by

$$g = dr^2 + m^2(r) d\theta^2, \quad m^2(r) = \frac{\cos^2 r}{1 - \lambda \cos^2 r}, \quad \lambda = 4/5.$$

Moreover, since θ is a cyclic variable, then $\mathbf{G} = p_\theta$ is an additional first integral given by the Clairaut relation. Trajectories of $\vec{\mathbf{H}}$ split into three cases: the *meridians* defined by $\theta = \text{constant}$ with $p_\theta = 0$, the equator identified to $r = 0$ with $p_\theta = m(r)$, and remaining geodesics with $|p_\theta| \in (0, m(r))$ formed by r -periodic oscillating solutions of the mechanical system, defined by the so-called *characteristic equation*

$$\left(\frac{dr}{dt} \right)^2 = 1 - V(r, p_\theta) = R(r, p_\theta),$$

the term $V(r, p_\theta) = \frac{p_\theta^2}{m^2(r)}$ representing the *potential*. A further integration is necessary in order to recover the θ -variable using the Hamiltonian dynamics. Parameterizing by r on each ascending branch of the characteristic equation, we have:

$$\frac{d\theta}{dr} = \frac{1}{\sqrt{R(r, p_\theta)}} \frac{\partial \mathbf{H}}{\partial p_\theta}.$$

This allows to compute the variation denoted $\Delta\theta/2$ of the angle θ starting from the equator and on the ascending branch, the total variation to return to the equator being $\Delta\theta$. Note that in the limit case of the

equator solution, the rotation is stationary since r is constant. This gives the complete description of the Liouville torus T^2 defined in Theorem 4.1 hereinafter. Note that the geodesics split into periodic orbits if $\Delta\theta/2\pi$ is *rational* and dense orbits in the Liouville Torus if $\Delta\theta/2\pi$ is *irrational*.

Theorem 4.1. (See [6, Section 1.4] and [2, Chapter 10]) *Let \vec{H} be a Hamiltonian vector field on T^*M (M being 2-dimensional) and assume that there exists a first integral G such that $\{H, G\} = 0$. Assume also that the vector fields \vec{H} and \vec{G} are complete and moreover that H and G are functionally independent on T^*M , i.e., their gradients are linearly independent on T^*M almost everywhere. Then, the Hamiltonian vector field \vec{H} is called Liouville-integrable. Let consider the level surface $T_\xi = \{(x, p) \in T^*M \mid H(x, p) = \xi_1, G(x, p) = \xi_2\}$ with $\xi = (\xi_1, \xi_2)$. Then:*

1. T_ξ is a smooth Lagrangian manifold invariant by the flow of \vec{H} and \vec{G} .
2. If T_ξ is connected and compact, then T_ξ is diffeomorphic to the 2-dimensional torus T^2 (called Liouville torus).
3. The Liouville foliation is trivial, that is, there exists a neighborhood U of T_ξ such that U is the direct product of the torus T^2 and the disk D^2 .
4. In the neighborhood U there exists symplectic coordinates (s, φ) (also called action-angle variables) such that the dynamics \vec{H} can be written in the form $\frac{ds_i}{dt} = 0, \frac{d\varphi_i}{dt} = \alpha_i(s_1, s_2), i = 1, 2$, and for which the motion is quasi-periodic.

Next, we present a generalization of the previous mechanical representation in the Zermelo case.

4.2 Mechanical representation in the Zermelo case

In this case, since we have a current, there is no longer equivalence between the time and energy minimization problems. So, we consider the Hamiltonian associated to the time minimization problem given by

$$\mathbf{H}(z) = H_0(z) + \|p\|_g + p^0 = \mu(r)p_\theta + \left(p_r^2 + \frac{p_\theta^2}{m^2(r)}\right)^{\frac{1}{2}} + p^0.$$

The following theorem sets the framework for the classification of the geodesic flow.

Theorem 4.2. *Consider a Zermelo navigation problem on a surface of revolution with parallel current. Then:*

1. *The evolution of the system in the (r, p_r) -space is described by the Hamiltonian dynamics*

$$\frac{dr}{dt} = \frac{p_r}{\|p\|_g}, \quad \frac{dp_r}{dt} = -p_\theta \mu'(r) + \frac{p_\theta^2 m'(r)}{m^3(r) \|p\|_g}. \quad (22)$$

2. *Restricted dynamics (22) can be integrated using the mechanical system representation*

$$\left(\frac{dr}{dt}\right)^2 + V_\varepsilon(r, p_\theta) = 1,$$

where the generalized potential is given by

$$V_\varepsilon(r, p_\theta) = \frac{p_\theta^2}{m^2(r)(\varepsilon + p_\theta \mu(r))^2}$$

with $\varepsilon = p^0$ normalized to $-1, 0, +1$ respectively in the hyperbolic, abnormal and elliptic cases.

3. *Moreover, the following relation holds*

$$p_r^2 = (\varepsilon + p_\theta \mu(r))^2 - \frac{p_\theta^2}{m^2(r)}.$$

Proof. Item 1 is a direct computation of eq. (4) considering the Hamiltonian defined above. Moreover, since the Hamiltonian $\mathbf{H} = \|p\|_g + p_\theta \mu(r) + p^0 = 0$ and $\|p\|_g = \left(p_r^2 + \frac{p_\theta^2}{m^2(r)}\right)^{1/2}$, we have:

$$p_r^2 = \|p\|_g^2 - \frac{p_\theta^2}{m^2(r)} = (\varepsilon + p_\theta \mu(r))^2 - \frac{p_\theta^2}{m^2(r)},$$

which gives item 3. Besides, from the restricted Hamiltonian system in (r, p_r) we have:

$$\left(\frac{dr}{dt}\right)^2 = \frac{p_r^2}{\|p\|_g^2} = \frac{(\varepsilon + p_\theta \mu(r))^2 - \frac{p_\theta^2}{m^2(r)}}{(\varepsilon + p_\theta \mu(r))^2} = 1 - \frac{p_\theta^2}{m^2(r) (\varepsilon + p_\theta \mu(r))^2},$$

which gives item 2. □

Definition 4.1. *The classification of trajectories of the restricted Hamiltonian dynamics (22), parameterized by p_θ is called the Generalized-Morse-Reeb (GMR) classification defined by the generalized potential V_ε .*

Orbits are classified according to the following definitions.

Definition 4.2. *We consider the hyperbolic case $\varepsilon = -1$. A pair (r^*, p_θ^*) is called an equator if $(r^*, 0)$ is an equilibrium point of the restricted Hamiltonian dynamics, parameterized by p_θ^* . It is called L-elliptic if the linearized dynamics is with spectrum $\{\pm i\alpha, \alpha \neq 0\}$, L-hyperbolic if the spectrum is of the form $\{\pm\lambda, \lambda \in \mathbb{R} \setminus 0\}$ and L-parabolic if the spectrum is zero. The L-elliptic and L-hyperbolic situations correspond respectively to a stable case associated to a minimum of the potential and to an unstable case associated to a maximum. An equator defines a stationary rotation in the (r, θ) -space, it is called a positive (resp. negative) rotation if θ is rotating with a positive (resp. negative) frequency. A separatrix geodesic parameterized by p_θ^* is a geodesic $(r(t), \theta(t))$ such that $r(t) \rightarrow r^*$ as $t \rightarrow \infty$ where (r^*, p_θ^*) is an equator.*

We give next some characterizations of equators and separatrices.

Proposition 4.1. *Consider the hyperbolic case $\varepsilon = -1$.*

1. *A pair (r^*, p_θ^*) is an equator if and only if it is a solution of:*

$$V_\varepsilon(r, p_\theta) = 1 \quad \text{and} \quad \frac{\partial V_\varepsilon}{\partial r}(r, p_\theta) = 0. \quad (23)$$

2. *An equator (r^*, p_θ^*) is L-hyperbolic (resp. L-elliptic) if and only if:*

$$\frac{\partial^2 V_\varepsilon}{\partial r^2}(r^*, p_\theta^*) < 0 \quad (\text{resp.} \quad \frac{\partial^2 V_\varepsilon}{\partial r^2}(r^*, p_\theta^*) > 0).$$

3. *A separatrix geodesic is necessarily associated to a L-hyperbolic equator and if we denote by (r^*, p_θ^*) this equator, then we have:*

$$p_\theta^* = \frac{m(r^*)}{\mu(r^*)m(r^*) + \delta} \quad \text{with} \quad \delta = \text{sign}(p_\theta^*).$$

Proof. If (r^*, p_θ^*) is an equator, then by definition $\dot{r} = \dot{p}_r = 0$, that is $p_r = \dot{p}_r = 0$ and so also $p_\theta^* \neq 0$. Besides,

$$\begin{aligned} p_r = 0 &\iff p_r^2 = (\varepsilon + p_\theta \mu(r))^2 - \frac{p_\theta^2}{m^2(r)} = 0 \\ &\iff (\varepsilon + p_\theta \mu(r))^2 = \frac{p_\theta^2}{m^2(r)} \\ &\iff V_\varepsilon = 1 \quad \text{if} \quad p_\theta \neq 0. \end{aligned}$$

On the other hand:

$$\begin{aligned}
\frac{\partial V_\varepsilon}{\partial r}(r, p_\theta) &= \frac{-2p_\theta^2 m(r) \mu'(r) - 2p_\theta^3 m'(r)(\varepsilon + p_\theta \mu(r))}{m^3(r)(\varepsilon + p_\theta \mu(r))^3} \\
&= \frac{2p_\theta^3 \mu'(r)}{m^2(r) \|p\|_g^3} - \frac{2p_\theta^2 m'(r)}{m^3(r) \|p\|_g^2}, \quad \text{using } \|p\|_g = -(\varepsilon + p_\theta \mu(r)) \\
&= \frac{2}{\|p\|_g} \left(p_\theta \mu'(r) - \frac{p_\theta^2 m'(r)}{m^3(r) \|p\|_g} \right), \quad \text{using } (\varepsilon + p_\theta \mu(r))^2 = \frac{p_\theta^2}{m^2(r)} \\
&= \frac{2}{\|p\|_g} \dot{p}_r.
\end{aligned}$$

This proves item 1. For the item 2, denoting $\lambda = (r, p_r)$, $f = (f_1, f_2) = \left(\frac{p_r}{\|p\|_g}, -p_\theta \mu'(r) + \frac{p_\theta^2 m'(r)}{m^3(r) \|p\|_g} \right)$ and $A = f'(r^*, 0)$ the differential of f at $(r^*, 0)$, then the linearized dynamics around $(r^*, 0)$ reads:

$$\dot{\delta \lambda} = A \delta \lambda \quad \text{with} \quad A = \begin{pmatrix} \frac{\partial f_1}{\partial r}(r^*, 0) & \frac{\partial f_1}{\partial p_r}(r^*, 0) \\ \frac{\partial f_2}{\partial r}(r^*, 0) & \frac{\partial f_2}{\partial p_r}(r^*, 0) \end{pmatrix} = \begin{pmatrix} 0 & \frac{1}{m^2(r^*)} \\ \frac{\partial \dot{p}_r}{\partial r}(r^*, 0) & 0 \end{pmatrix}.$$

Indeed,

$$\frac{\partial f_1}{\partial r} = \frac{\partial f_2}{\partial p_r} = \frac{m'(r) p_r p_\theta^2}{m^3(r) \|p\|_g^3} \quad \text{and} \quad \frac{\partial f_1}{\partial p_r} = \frac{p_\theta^2}{m^2(r) \|p\|_g^3} \quad \text{since} \quad \|p\|_g^2 - p_r^2 = \frac{p_\theta^2}{m^2(r)}.$$

Thus, $\text{sign}(\det A) = -\text{sign}\left(\frac{\partial \dot{p}_r}{\partial r}(r^*, 0)\right)$, since $\frac{1}{m^2(r^*)} > 0$. On the other hand, one has

$$\frac{\partial V_\varepsilon}{\partial r}(r, p_\theta) = \frac{2}{\|p\|_g} \dot{p}_r \quad \implies \quad \frac{\partial^2 V_\varepsilon}{\partial r^2}(r, p_\theta) = \frac{2}{\|p\|_g} \frac{\partial \dot{p}_r}{\partial r} - \frac{2 \dot{p}_r}{\|p\|_g} \frac{\partial \|p\|_g}{\partial r}$$

but since $\dot{p}_r = 0$ at $(r^*, 0)$, then $\text{sign}\left(\frac{\partial^2 V_\varepsilon}{\partial r^2}(r^*, p_\theta^*)\right) = \text{sign}\left(\frac{\partial \dot{p}_r}{\partial r}(r^*, 0)\right)$ and thus

$$\text{sign}(\det A) = -\text{sign}\left(\frac{\partial^2 V_\varepsilon}{\partial r^2}(r^*, p_\theta^*)\right).$$

Item 2 then follows. For item 3, let us remark that the first equation of (23) is equivalent to $p_r = 0$ along the curve, and resolving this equation leads us to

$$p_\theta = \frac{m'(r)}{m(r) \mu'(r) + m'(r) \mu(r)}.$$

On the other hand, $p_r = 0$ along the curve implies $\dot{p}_r = 0$ which gives

$$\mu'(r) = \delta \frac{m'(r)}{m^2(r)} \quad \text{where} \quad \delta = \text{sign}(p_\theta).$$

These two equations then lead us to

$$p_\theta = \frac{m(r)}{\mu(r) m(r) + \delta}.$$

Proposition then follows. \square

Definition 4.3. *Let U be an adapted rectangular neighborhood of q_0 . Geodesics starting from q_0 decompose into starting ascending or descending r -branches. At the limit tangential case, monotonicity is given by positive or negative acceleration $\frac{d^2 r}{dt^2}(0)$. The first return to the equator (resp. the meridian) associated to a geodesic is the first point such that the geodesic intersects again the equator (resp. the meridian).*

Proposition 4.2. *Let U be a rectangular adapted neighborhood of $q_0 = (r_0, \theta_0)$. Level sets of the Hamiltonian in the GMR-classification split into compact levels corresponding to r -periodic geodesics and non-compact level sets corresponding to r -aperiodic geodesics, when the dynamics is restricted to the neighborhood U . If (r^*, p_θ^*) is a L -elliptic equator, then locally the Liouville foliation by Liouville torus is preserved.*

Remark 4. *Let q_0 be a fixed initial condition, then using the GMR-classification for each adapted rectangular neighborhood of q_0 we can stratify the set of geodesics emanating from q_0 into micro-local conic sectors corresponding to compact and non-compact geodesics.*

Remark 5. *The decomposition depends upon the adapted rectangular neighborhood and can be described using the generalized potential restricted to the domain. we can easily have situations with two compact sectors separated by a singular level with a separatrix geodesic, or an equator for which when restricted to the domain, the singular level separates compact and non-compact orbits. This property can be illustrated for example in the Serret-Andoyer case, described in details in [11]. In this case the meridian can be identified to $r = 0$ and starting from the meridian, geodesics split into r -periodic curves and r -aperiodic curves with a limit curve corresponding to a separatrix. Only r -periodic curves have conjugate points. They are a representation of the standard pendulum equation where the oscillating solutions correspond to r -periodic solution while rotating solutions correspond to r -aperiodic solutions. But if they are interpreted on the cylinder, both types of solutions are periodic, oscillating trajectories are homotopic to a point, but not the rotating ones.*

5 Case studies

5.1 The averaged Kepler case

The aim of this section is to analyze the Zermelo navigation problem associated to the Riemannian case studied in [7, 8]. We first recap the properties of the Zermelo problem associated to the Riemannian metric, when the current is zero and then extend the results to the Zermelo case with strong current.

5.1.1 Riemannian case

Recall that the metric takes the form $g = d\varphi^2 + m_\lambda^2(\varphi) d\theta^2$, with

$$m_\lambda^2(\varphi) = \frac{\sin^2 \varphi}{1 - \lambda \sin^2 \varphi}, \quad (24)$$

where φ represents the angle on the two-sphere of revolution, where $\varphi = 0$ (resp. $\varphi = \pi$) corresponds to the north (resp. south) pole and $\lambda \in [0, 1]$ is an homotopic parameter, $\lambda = 0$ being the *round sphere*, $\lambda = 4/5$ is associated to Kepler orbits transfer and $\lambda = 1$ is the so-called *Grushin case* with a singularity at the equator.

The Gauss curvature is given by

$$K_\lambda = \frac{1}{(1 - \lambda \sin^2 \varphi)^2} ((1 - \lambda) - 2\lambda \cos^2 \varphi),$$

and is strictly negative in the limit case $\lambda = 1$. The only equator solution corresponds to $\varphi = \pi/2$ and we introduce $r = \pi/2 - \varphi$ to normalize this equator to zero. The metric is then written $g = dr^2 + m^2(r) d\theta^2$, where we set $m(r) = m_\lambda(\pi/2 - r)$ and it is symmetric with respect to the equator, that is $m(r) = m(-r)$, which is crucial for the explicit computations of the conjugate and cut loci, following[9]. Using the Hamiltonian formalism we associate to the metric the Hamiltonian

$$\mathbf{H} = \frac{1}{2} \left(p_r^2 + \frac{p_\theta^2}{m^2(r)} \right) + p^0.$$

Fixing the parameterization to the arc-length amounts to set $p^0 = -1$. So that the characteristic equation takes the form:

$$\left(\frac{dr}{dt} \right)^2 + V(r, p_\theta) = 1 \quad \text{with} \quad V(r, p_\theta) = \frac{p_\theta^2}{m^2(r)}.$$

A geodesic is either a meridian if $p_\theta = 0$, the equator if $p_\theta = m(r)$ and any solution is such that r is periodic and oscillates between $-r_+$, r_+ and is entirely determined by a branch of the characteristic equation evaluated

on the quarter of period $T/4$, $r(t)$ being restricted to $[0, r_+]$, where r_+ is the positive root of the equation $V = 1$, the period being given by the integral

$$T = 4 \int_0^{r_+} \frac{dr}{(1 - V(r, p_\theta))^{1/2}},$$

which depends upon p_θ . By symmetry with respect to the equator it can be supposed non-negative and belonging to $(0, m(r(0)))$. To make the analysis we introduce the application called the *period mapping* associated to the first return to the equator and defined by: $p_\theta \mapsto T(p_\theta)$.

The geodesic flow is integrated by quadrature using the characteristic equation and the transcendence of the solutions is basically determined by the transcendence of the period mapping. In this context, this case study is rather straightforward, since only elementary functions are necessary to parameterize the solutions. In particular, it is related to the historical example, replacing the ambient Euclidean space by a two-sphere. To integrate, we can assume that $r(0) = 0$ and $\theta(0) = 0$, since every oscillating trajectory is such that r is intersecting the equator and we use:

$$\frac{dr}{dt} = \sqrt{1 - V(r, p_\theta)}, \quad \frac{d\theta}{dt} = \frac{\partial H}{\partial p_\theta} = \frac{V(r, p_\theta)}{p_\theta}.$$

One gets that

$$\theta(t) = (2n - 1)\Delta\theta + \int_{r(t)}^0 \frac{V(r, p_\theta)}{p_\theta(1 - V(r, p_\theta))^{1/2}} dr,$$

where $n \in \mathbb{N}$ counts the number of intersections with the equator and by symmetry, we can assume that the number of intersections is odd. The function $\Delta\theta$ for $p_\theta \in (0, m(0))$ is the first return mapping to the equator introduced in Definition 4.3. The following proposition coming from [9] is crucial in the optimality analysis.

Proposition 5.1. *Restricting the initial point to $q_0 = (0, 0)$ and assuming that the first return mapping to the equator is tame, that is monotone non-increasing, then the first conjugate time is given by the equation*

$$\frac{\partial \theta}{\partial p_\theta}(r, p_\theta) = 0,$$

where θ is parameterized by r according to

$$\theta(r, p_\theta) = \Delta\theta(p_\theta) - \int_{r_+}^r \frac{V(\rho, p_\theta)}{p_\theta \sqrt{1 - V(\rho, p_\theta)}} d\rho,$$

and the first conjugate time being between $T/2$ and $T/2 + T/4$.

Integration of the geodesics. We take

$$\left(\frac{dr}{dt}\right)^2 = \frac{\cos^2 r - p_\theta^2(1 - \lambda \cos^2 r)}{\cos^2 r},$$

and we denote by Z_+ and Z_- the roots of $1 + p_\theta^2(\lambda - 1) = Z^2(1 + \lambda p_\theta^2)$, where $Z = \sin r$ and the period reads

$$\frac{T}{4} = \int_0^{Z_+} \frac{dZ}{\sqrt{1 + p_\theta^2(\lambda - 1) - Z^2(1 + \lambda p_\theta^2)}}.$$

Normalizing the amplitude of the oscillation by $Z = Z_+ Y$ one has

$$\frac{T}{4} = \int_0^1 \frac{dY}{\sqrt{(1 + \lambda p_\theta^2)(1 - Y^2)}}.$$

Proposition 5.2. *The period is given by*

$$T(p_\theta) = \frac{2\pi}{\sqrt{1 + \lambda p_\theta^2}}.$$

Moreover we have $\arcsin Y(t) = \sqrt{1 + \lambda p_\theta^2} t$.

This defines the re-normalized time $s = \sqrt{1 + \lambda p_\theta^2} t$ and the θ -variable is integrated using

$$\frac{d\theta}{ds} = p_\theta \frac{1 - \lambda(1 - \sin^2 r)}{1 - \lambda \sin^2 r}.$$

A quadrature gives the following. The θ -dynamics is given by

$$\theta(t) = \frac{p_\theta}{\sqrt{(1 + \lambda p_\theta^2)(1 - Z_+^2)}} \operatorname{atan} \left(\tan \left((1 + \lambda p_\theta^2)t \sqrt{1 - Z_+^2} \right) \right) - \lambda p_\theta t.$$

This leads to a complete parameterization of the geodesics. Moreover, we can compute explicitly the conjugate and cut loci in the tame case according to the following propositions.

Proposition 5.3. *In the tame case, the cut locus of a point on the equator is a sub-arc of the equator and the injectivity radius is the distance to the cusp extremity of the conjugate locus on the equator.*

Proposition 5.4. *Assume that the problem is tame and moreover, suppose that the first return mapping $\Delta\theta$ is such that $\Delta\theta' < 0 < \Delta\theta''$ on $(0, m((r(0))))$, then:*

1. *The cut locus of a point not a pole is a segment of the antipodal parallel.*
2. *For a point not a pole, the conjugate locus has exactly four cusp points.*

Computing, we have.

Proposition 5.5. *For $\lambda \in (0, 1)$, the Riemannian metric where m_λ is given by (24) is such that the problem is tame and moreover $\Delta\theta' < 0 < \Delta\theta''$ on $(0, m((r(0))))$, so that the assertions of Proposition 5.4 hold.*

This can be applied to our case for $\lambda \in (0, 1)$. Note also that the conjugate locus of the equator is a standard astroid with four cusps. The limit Grushin case $\lambda = 1$ can be analyzed similarly, except that the equator is not a geodesic and the injectivity radius is zero. This gives a complete analysis of the Riemannian case and this leads to the following analysis.

5.1.2 Transition from the Riemannian case to the Zermelo case with a constant current

Recall that the problem with constant current is given on the covering space by the pair

$$F_0 = v \frac{\partial}{\partial \theta}, \quad g = dr^2 + m^2(r) d\theta^2,$$

where v is a non-zero constant. Depending on the current at the initial point $q_0 = (r_0, \theta_0)$, we say that we are in the *weak (current) case* if $\sin^2 r_0 < \frac{1}{v^2 + \lambda}$, *strong case* if $\sin^2 r_0 > \frac{1}{v^2 + \lambda}$ and *moderate case* if $\sin^2 r_0 = \frac{1}{v^2 + \lambda}$. In the case where $v^2 + \lambda < 1$, the current will be weak on the whole domain. So we shall assume: $v^2 + \lambda > 1$. The following is a crucial geometric property.

Proposition 5.6. *On the two-sphere of revolution embedded in \mathbb{R}^3 , the vector field F_0 defines a linear vector field, tangent to the sphere, and it corresponds to a uniform rotation whose axis is the axis of revolution. For the metric the equator solution is also a stationary rotation since $\frac{d\theta}{dt}$ is constant so that the effect of the current can be added to this rotation.*

Integration of the geodesics. From the previous proposition, the integration follows from the Riemannian case. Introducing the generalized potential, recall that the r -dynamics is given by:

$$\left(\frac{dr}{dt} \right)^2 + V_\varepsilon(r, p_\theta) = 1$$

where $\varepsilon = p^0 < 0, = 0, > 0$ correspond respectively to the hyperbolic, abnormal and elliptic cases. Taking the ascending branch starting from the equator $r_0 = \pi/2$, we have

$$\frac{dr}{dt} = \left(\frac{p_\theta^2(1 - \lambda \sin^2 r)}{\sin^2 r(\varepsilon + p_\theta v)^2} \right)^{1/2},$$

Since $H = 0$, $\|p\|_g = -(p_\theta v + \varepsilon)$, then, using a time reparameterization, one gets:

$$\frac{dr}{ds} = \left(\frac{p_\theta^2 (1 - \lambda \sin^2 r)}{\sin^2 r} \right)^{1/2},$$

which is like the r -dynamics in the Riemannian case, with the addition of v . Then, we can determine the first return mapping to the equator $r_0 = \pi/2$:

$$\frac{\Delta\theta}{2} = \int_{\pi/2}^{r_+} \frac{\partial H / \partial p_\theta}{\partial H / \partial p_r} dr$$

where r_+ is the maximum of $r(t)$.

Again the geodesic curves are symmetric with respect to the equator, the cone of admissible direction being symmetric with respect to the equator. This leads to the following stratification of the set of geodesics, using the variable p_θ instead of the heading angle in the historical example.

Proposition 5.7. *Assume that $\lambda = 4/5$ and $v = 0.9$, then starting from the equator and considering only the ascending branch, geodesics split into:*

- Abnormal given by $p_\theta^a = -1/v$;
- Hyperbolic geodesics parameterized by $p_\theta \in (p_\theta^a, m(r_0))$;
- Elliptic geodesics parameterized by $p_\theta \in (-m(r_0), p_\theta^a)$.

Moreover, in the hyperbolic case, the set of geodesics can be stratified in four different classes (see Fig. 5 for illustration):

- The equator which corresponds to $r = \pi/2$, $p_r = 0$ and $p_\theta = m(r_0)$.
- The two pseudo-meridians (ascending and descending ones) which correspond, on the covering space, to non-compact case where $p_\theta = 0$.
- Generic r -periodic orbits which split in two different families namely orbits without self-intersections, parameterized by $p_\theta \in (0, m(r_0))$ and orbits with self-intersections, parameterized by $p_\theta \in (p_\theta^a, 0)$ and $\pm p_r(0)$ corresponding to the symmetric orbits.

Remark 6. *The other geodesics in the flow are obtained by a symmetry which respect to the equator.*

The cut locus in this case will split into two branches. The first branch is associated as in the historical example to the cusp singularity of the abnormal directions, which are symmetric with respect to the equator (see Fig. 6 for an illustration). The second branch of the cut locus is the persistence of the segment formed by the equator and related to the tame behavior of the first return mapping corresponding to non self-intersecting geodesics. The conjugate points can be numerically evaluated. They exist for different types of geodesics but occur after the intersection of the geodesics with the equator.

Theorem 5.1. *Assume that the equator $r_0 = \pi/2$ is in the strong current domain. Then the cut locus has two branches, the first branch being formed by the abnormal curves occurring in the neighborhood of the cusp point and associated to self-intersecting geodesics and the second branch being a segment of the equator, starting by a cusp point of the conjugate locus and associated to non self-intersecting geodesics.*

5.2 Complexity of the Hamiltonian dynamics in the generalized vortex case

A preliminary study of a navigation problem with a vortex localized at the origin is studied in [13], but the aim of this section is to generalize this situation to get more intricate dynamics, in relation with the N-body problem. A first step is to generalize the existence theorem to get a geodesically complete framework.

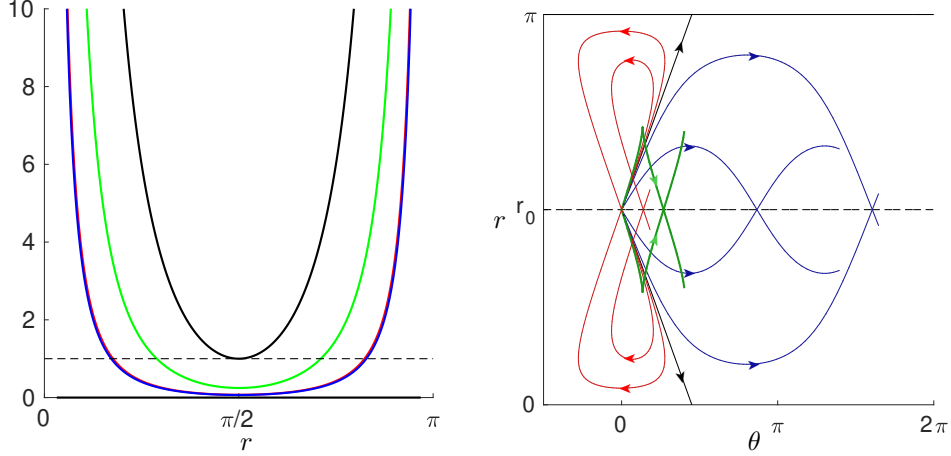


Figure 5: (Left) Potential for the different classes of geodesics. (Right) Different types of hyperbolic geodesics in the strong current case. The meridians are represented in black and hyperbolic geodesics with self-intersection (resp. without self-intersection) are represented in red (resp. in blue). Abnormal geodesics are represented in green. We take $\lambda = 4/5$ and $v = 0.9$.

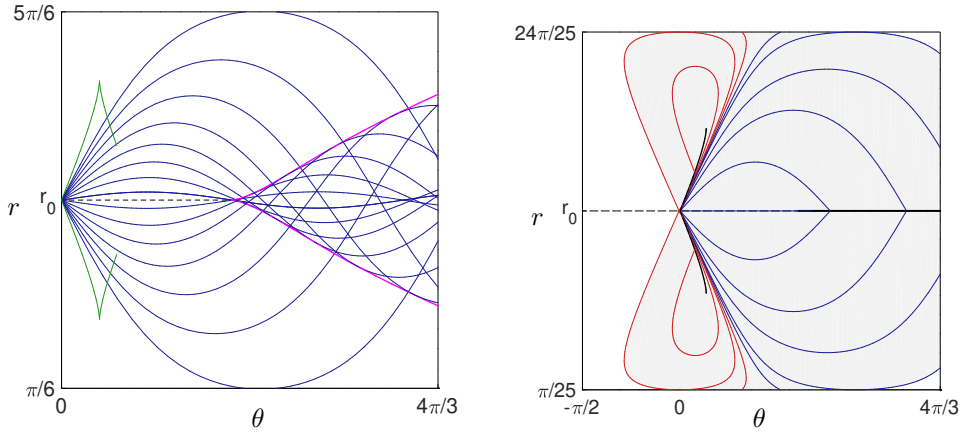


Figure 6: (Left) Illustration of the hyperbolic flow and of a part of the conjugate locus. (Right) Optimal synthesis in minimal time in the adapted neighborhood $R = \{\pi/25 \leq r \leq 24\pi/25; -\pi/2 \leq \theta \leq 4\pi/3\}$. In thick black is represented the cut locus. The gray sector represents, in the considered neighborhood, the accessible domain from the equator by geodesics. The white domain is not accessible from the equator by a geodesic in this neighborhood. We take $\lambda = 4/5$ and $v = 0.9$.

5.2.1 Existence of optimal solutions

We consider the case where the Zermelo navigation problem is defined by:

$$F_0 = \mu(r) \frac{\partial}{\partial \theta}, \quad F_1 = \frac{\partial}{\partial r}, \quad F_2 = \frac{1}{m(r)} \frac{\partial}{\partial \theta}.$$

In our preliminary study, we have $\mu(r) = \frac{k}{r^2}$ but in the general case we shall assume that $\mu(r)$ has a pole of order $\beta \in (1, +\infty)$ at zero, so that near zero, we can take the approximation $\mu(r) \sim \frac{1}{r^\beta}$ and moreover we assume that $\mu(r) \rightarrow 0$ as $r \rightarrow +\infty$. We shall generalize the argument of [13] and relate the proof to existence of minimizing solutions avoiding collisions in the N-body problem [21]. Also, we point the relation between extending the solutions beyond the vortex and the Levi-Civita regularization for double collision [29].

Theorem 5.2. *Take q_0, q_1 in the punctured plane $\mathbb{R}^2 \setminus \{0\}$, then there exists a time minimizing trajectory to transfer q_0 to q_1 . Moreover, $q_0 = (r_0, \theta_0)$ can be transferred to the origin in minimum time $t_{\min} = r_0$. Hence,*

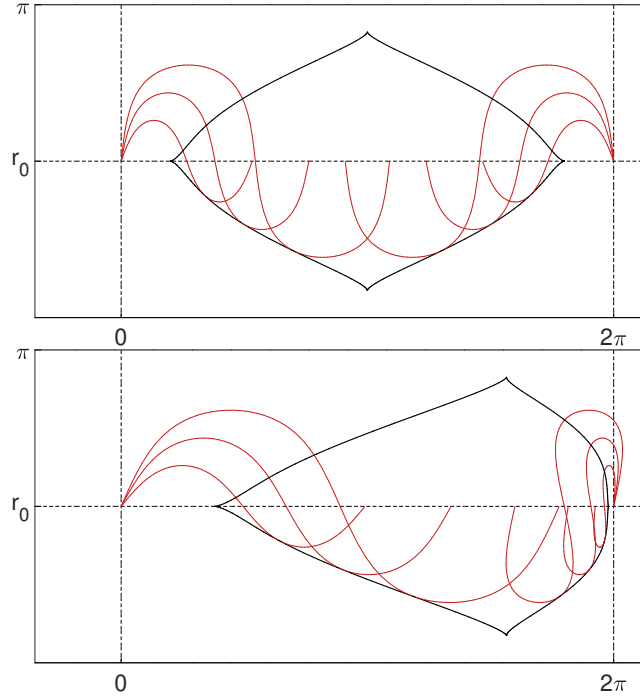


Figure 7: Deformation of the geodesic flow and conjugate locus starting from the Riemannian case to the strong Zermelian case. We take $\lambda = 4/5$ and $v = 0.0, 0.4, 0.8$, respectively in the Riemannian (top), Finslerian (bottom) and Zermelian (Fig. 8) cases. In red is represented the hyperbolic geodesics. Conjugate locus for the hyperbolic geodesics is represented in black.

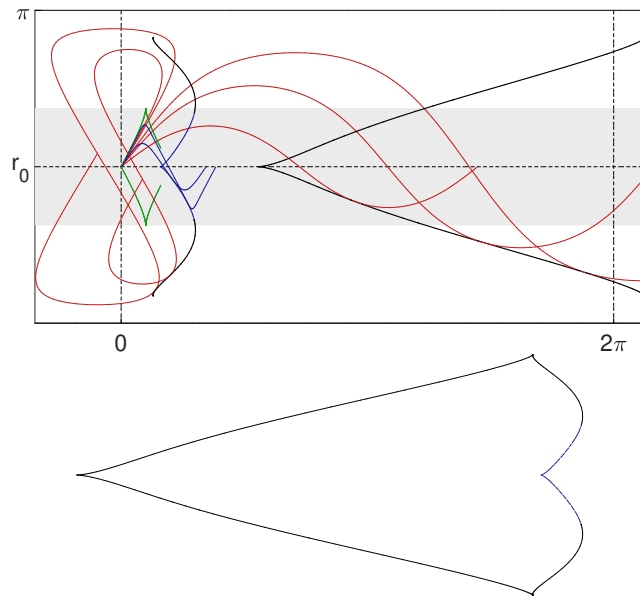


Figure 8: Deformation of the geodesic flow and conjugate locus starting from the Riemannian case to the strong Zermelian case. We take $\lambda = 4/5$ and $v = 0.0, 0.4, 0.8$, respectively in the Riemannian (Fig. 7 top), Finslerian (Fig. 7 bottom) and Zermelian (top) cases. In red (resp. in blue) is the hyperbolic (resp. elliptic) geodesics. Conjugate locus for the hyperbolic (resp. elliptic) geodesics is represented in black (resp. in dashed blue). The gray sector represents the strong current domain. Note that the conjugate locus is a closed curve on the manifold, cf. the bottom figure.

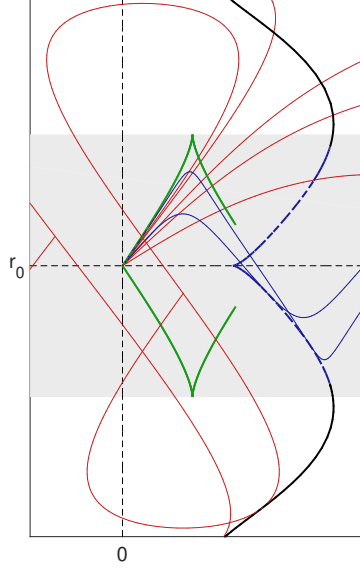


Figure 9: Zoom of Fig. 8. We can see on this figure the connection between the elliptic and the hyperbolic conjugate locus.

we can extend the geodesic flow using a Levi-Civita type regularization beyond the collision with the pole by reversing the time parameterization when crossing the vortex.

Proof. The geodesic dynamics in polar coordinates reads

$$\frac{dr}{dt} = \frac{p_r}{\|p\|_g}, \quad \frac{d\theta}{dt} = \mu(r) + \frac{p_\theta}{m^2(r)\|p\|_g}.$$

As in [13], to prove the existence about minimizing trajectories it is sufficient to prove that the minimizing trajectories avoid the collision. Using the expansion near the pole and comparing the time to make a rotation around the pole on a circle of radius r denoted $T_\theta(r)$ and the minimal time to reach a circle of radius ε denoted $T_r(\varepsilon)$ a direct computation gives

$$T_\theta(r) = \frac{2\pi r^\beta m(r)}{r + m(r)}, \quad T_r(\varepsilon) = r - \varepsilon.$$

Hence, the argument of [13] to replace a trajectory reaching a circle with small radius ε by the trajectory making a rotation around the pole (see Fig. 10) is still valid and the existence result follows. Clearly from the equations the time to reach the pole from q_0 is obtained for $p_\theta = 0$ and is given by r_0 . Following the Levi-Civita regularization we reverse the geodesics orientations when crossing the vortex. It amounts in particular to replace $\mu(r)$ by $-\mu(r)$ and p_θ by $-p_\theta$ in the geodesics equations. \square

Remark 7. To replace the pole of the vortex potential by $\beta > 1$ in the general vortex case is similar to the modification done by Poincaré in the Keplerian potential where he replaced the pole by $\beta \geq 2$ ($\beta \in \mathbb{N}$) in order to avoid collisions. In our case the bound of the pole is given by the conditions $T_\theta(r) < T_r(\varepsilon)$ i.e. $\varepsilon < r \left(1 - \frac{2\pi r^{\beta-1} m(r)}{r^\beta + m(r)} \right)$ and $0 < \varepsilon < r$.

5.2.2 The single vortex case in hydrodynamics

On the punctured plane we consider the case of an Euclidean metric in polar coordinates with

$$g = dr^2 + r^2 d\theta^2 \quad \text{and} \quad F_0 = \frac{k}{r^2} \frac{\partial}{\partial \theta}.$$

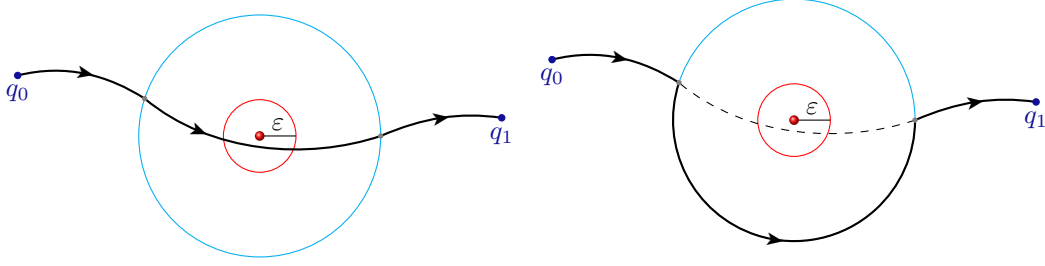


Figure 10: Illustration of the construction of a strictly better admissible trajectory. The vortex is represented by a red ball, while the trajectories are the solid black lines. We can see on the left, a trajectory crossing the ball of radius ε . This trajectory is replaced on the right picture by a strictly better admissible trajectory.

The generalized potential is given by

$$V_\varepsilon(r, p_\theta) = \frac{p_\theta^2 r^2}{(\varepsilon r^2 + p_\theta k)^2}.$$

The geodesic curves can be classified using the potential and the main features are described hereinafter. See [13] for more details and see also Figs. 11 and 12 for illustrations. We first introduce the following novel definition.

Definition 5.1. *A Reeb component is a foliation invariant by θ -rotation generated by a separatrix geodesic $(r(t), \theta(t))$ such that $r(t)$ converges when $t \rightarrow \pm\infty$ to two different equators, with different orientations.*

Then, in the single vortex case, we have the following results.

Proposition 5.8. *Considering the single vortex case, for a given $q_0 \in \mathbb{R}^* \setminus \{0\}$, we have:*

- *The domain of strong current is near the vortex and limited by the circle of radius $r = k$ of moderate current. The only equator solution is in the domain of weak current and is defined by the circle with radius $r^* = 2k$. There exists a unique separatrix emanating from the vortex and converging to the equator with $\frac{d\theta}{dt} = 0$ on the circle of radius $2k/\sqrt{3}$. This separatrix forms a Reeb component in the interior of the disk delimited by the equator, whose foliation as a singularity at the vortex.*
- *At the exterior of the circle of radius r^* there exists a unique separatrix emanating from the equator and converging to the infinity.*
- *The separatrices split the geodesic flow into trajectories that converge towards the vortex and those that go to infinity.*
- *There exists two pseudo-meridians converging with maximal radial speed either towards the vortex or to the infinity.*

5.2.3 Generalized single vortex case

In this section, we describe a generalization of the situation analyzed in Section 5.2.2 in which we have several equators and separatrices in relation with similar studied in dynamical systems, see for instance [22]. We assume $m = 1$ and $\mu(r)$ rational but complex dynamics can be obtained with this restriction. We consider a system with a current of the form:

$$F_0(q) = \mu(r) \frac{\partial}{\partial \theta} \quad \text{with} \quad \mu(r) = \frac{\lambda r + \beta}{r^3},$$

$\lambda, \beta \in \mathbb{R} \setminus \{0\}$, so that the generalized potential is now given by

$$V_\varepsilon(r, p_\theta) = \frac{p_\theta^2 r^4}{(\varepsilon r^3 + p_\theta(\lambda r + \beta))^2}.$$

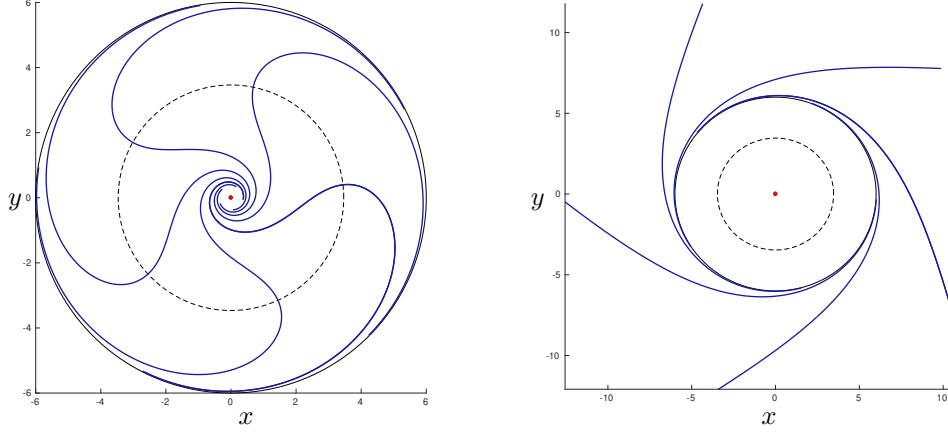


Figure 11: (Left) Reeb's foliation formed by the separatrices in the perforated disk of radius $2k$ in the (x, y) plane. (Right) Foliation formed by the separatrices outside the disk of radius $2k$. The vortex is placed at the origin and represented by a red point. The circles in black dotted lines correspond to the circle of radius $2k/\sqrt{3}$ (where $\dot{\theta}$ vanishes) and the circles in black plain lines correspond to the circle of radius $2k$.

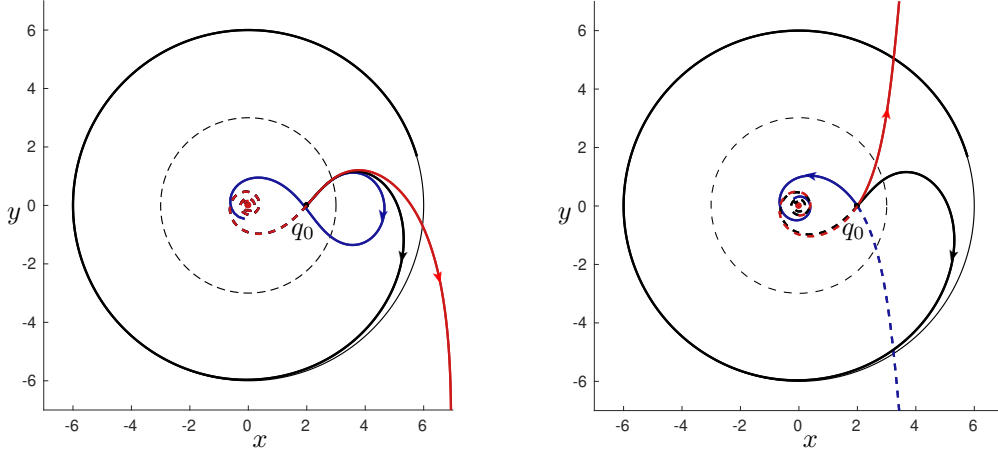


Figure 12: (Left) Behavior of the trajectories around the separatrix (black). The geodesics below the separatrix (blue), i.e. parameterized by $p_\theta < p_\theta^*$ (p_θ^* parameterizing the separatrix), converge towards the vortex and those above the separatrix (red) go to infinity. However, in the neighborhood of the separatrix the geodesics come from the vortex. (Right) Illustration of the two pseudo-meridians represented in red and blue. Note that both orbits do not coincide because of the drift. The dotted lines represent the semi-orbits computed backward in time.

Moreover we assume that $\lambda^2 > -3\beta$ and $\beta < 0$. To integrate the flow, as in the Kepler case, we first use the characteristic equation to integrate the r -dynamics. This leads us to

$$\frac{dr}{dt} = \sqrt{1 - V_\varepsilon(r, p_\theta)} = \left(\frac{(\varepsilon r^3 + p_\theta \lambda r + \beta)^2 - p_\theta r^4}{\varepsilon r^3 + p_\theta \lambda r + \beta} \right).$$

Then, we use an additional quadrature to integrate the θ -dynamics. Indeed, the θ dynamics given by $\frac{d\theta}{dt} = \frac{\partial \mathbf{H}}{\partial p_\theta}$ can be re-parameterized by

$$\frac{d\theta}{dr} = \frac{p_\theta \mu(r) + V_\varepsilon(r, p_\theta)}{(1 - V_\varepsilon(r, p_\theta))^{1/2}}.$$

Finally, the geodesic flow can be classified using the potential and the Clairaut parameter p_θ . At the end, we have the following.

Proposition 5.9. *Considering the generalized single vortex case and assuming that $\lambda^2 > -3\beta$ and $\beta < 0$, then we have:*

- There exist three equators $0 < r_1 < r_2 < r_3$ given by:

$$r_1 = -\lambda + \sqrt{\lambda^2 - 3\beta}, \quad r_2 = \lambda - \sqrt{\lambda^2 + 3\beta} \quad \text{and} \quad r_3 = \lambda + \sqrt{\lambda^2 + 3\beta}, \quad (25)$$

and respectively associated to the Clairaut constants:

$$p_\theta^1 = \frac{m(r_1)}{1 + \mu(r_1)m(r_1)}, \quad p_\theta^2 = -\frac{m(r_2)}{1 - \mu(r_2)m(r_2)} \quad \text{and} \quad p_\theta^3 = -\frac{m(r_3)}{1 - \mu(r_3)m(r_3)}.$$

The equators r_1 and r_3 are L-hyperbolic and the equator r_2 is L-elliptic. See Figs. 13 to 15 for illustrations and Definition 4.2.

- Equator r_1 forms a Reeb component delimited by the vortex and r_1 , as in the simple vortex case (see Fig. 13). while equator r_3 is an homoclinic trajectory (see Fig. 15).
- When $t \rightarrow +\infty$, the micro-local classification gives:
 - Equators r_1 and r_3 have two sectors formed by geodesics converging either to the vortex when $t \rightarrow +\infty$ or to infinity. The two sectors being delimited by a pseudo-meridian (see Fig. 16).
 - Equator r_2 has three sectors, two of them being as in the previous item, the third one corresponds to an elliptic sector (see Fig. 17).

5.3 Algorithm in the general case and the gluing process

5.3.1 Algorithm

We can deduce from the previous studies the method of analysis to handle a general case, and we proceed as follows. In the normal coordinates (r, θ) on the covering manifold M^c we have $r \in (0, R)$ and we can decompose the domain into disks $c_i < r < c_{i+1}$ with alternatively weak and strong currents. We compute the equators solutions listed as $0 < r_1 < r_2 < \dots < r_p < R$ and they can be classified according to their optimality status into L-hyperbolic or L-elliptic equators. Then, taking a point q_0 , we can parameterize the geodesics using the mechanical representation with the generalized potential using *improper integrals*. This allows to construct the *time minimal synthesis* fixing an *adapted neighborhood*, using the first return mappings to equators and meridians combined with conjugate point analysis, in both normal and abnormal cases. Note that in the strong current domain the size of the adapted neighborhood is defined by the limit loop of the self-intersecting geodesics related to the abnormal geodesics. This can be extended to a larger domain by gluing different adapted neighborhoods, see [30, 31] for such a procedure for general control problems in the plane.

5.3.2 The gluing process

In the previous section we describe the method to obtain global syntheses, by gluing together the syntheses using different adapted neighborhoods but intricate situations can be constructed starting from case studies by gluing such cases using the normal coordinates (r, θ) . Indeed, each case is described by a pair of covariant $(\mu_i(r), m_i(r))$, parameterizing respectively the current and the metric. They can be glued together in the \mathbb{C}^∞ -category using *bump functions*. For instance the vortex case with Euclidean metric can be glued to the averaged Kepler case, to represent the Zermelo navigation problem of a passive tracer, swallowed by the vortex to enter into a Kepler domain, to visit an equator solution, with non zero curvature and with different types of geodesics.

6 Conclusion

The main contribution of this article is starting from the historical navigation problem studied by Zermelo and Carathéodory to introduce general tools from geometric control to analyze navigation problems on surfaces of revolution, based on the inspection of the geodesic curves. Two complementary techniques have been introduced. First of all, the system can be extended to a single-input control system using the Goh-transformation and this extension is suitable to parameterize the geodesics by quadrature, using the heading angle of the ship

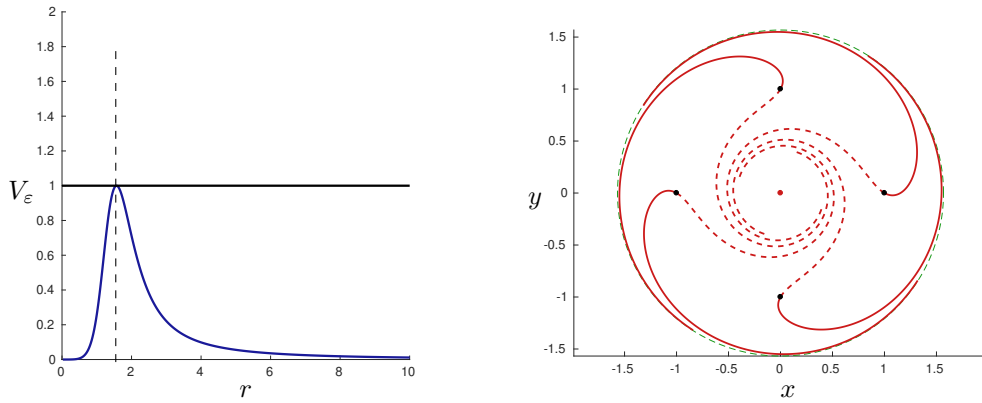


Figure 13: Reeb's foliation formed by the separatrix parameterized by p_θ^1 . (Left) The potential $r \mapsto V_\varepsilon(r, p_\theta^1)$, for $\varepsilon = -1$. (Right) In plain (resp. dashed) line, the trajectories are traveled in positive (resp. negative) time. The vortex is represented by the red dot and different initial points by the black dots. The green circle is the equator associated to r_1 .

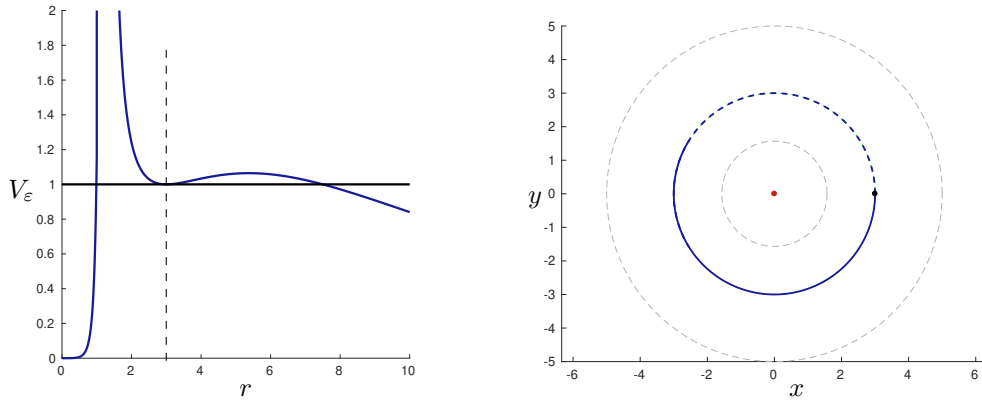


Figure 14: L-elliptic equator associated to r_2 . (Left) The potential $r \mapsto V_\varepsilon(r, p_\theta^2)$, for $\varepsilon = -1$. (Right) The green circle represents the equator associated to r_2 .

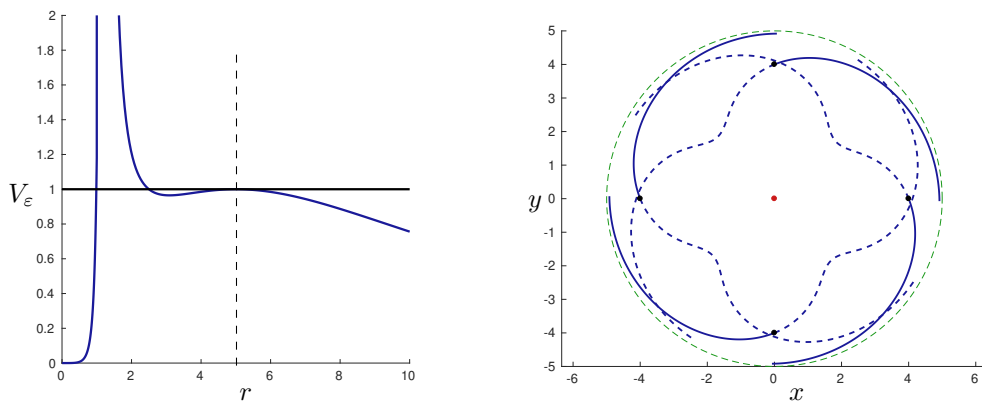


Figure 15: Homoclinic separatrix parameterized by p_θ^3 . (Left) The potential $r \mapsto V_\varepsilon(r, p_\theta^3)$, for $\varepsilon = -1$. (Right) The green circle represents the equator associated to r_3 .

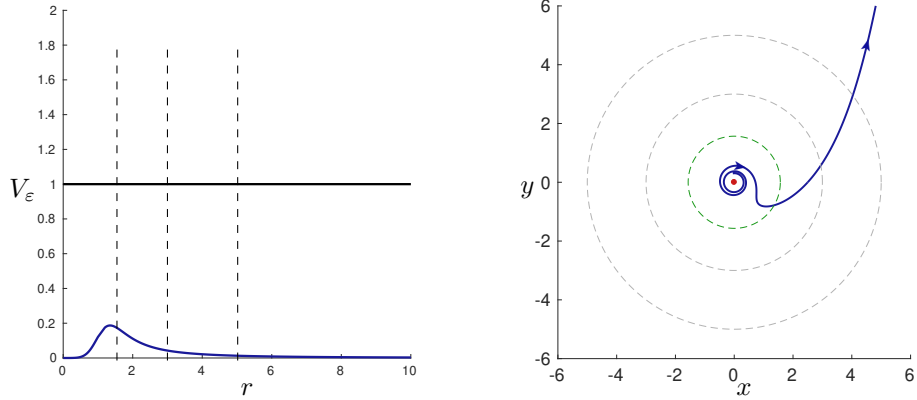


Figure 16: (Left) The potential $r \mapsto V_\varepsilon(r, p_\theta^1 + 0.1)$, for $\varepsilon = -1$. From the potential plot, one can deduce that the trajectories necessarily go to the vortex or to infinity.

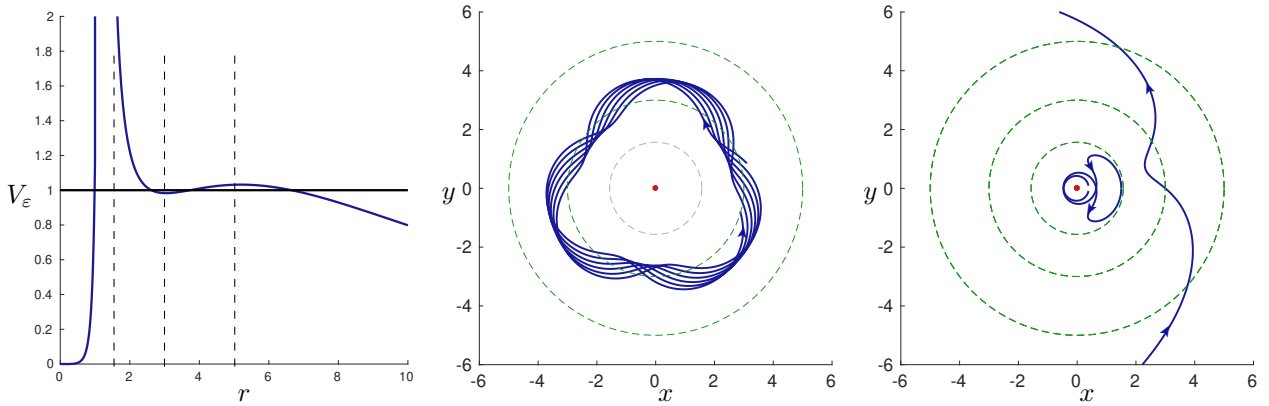


Figure 17: Different sectors around the L-elliptic equator r_2 . (Left) The potential $r \mapsto V_\varepsilon(r, p_\theta^2 - 0.3)$, for $\varepsilon = -1$. From the potential plot, we deduce that the trajectories starting close to r_2 remain contained in an annulus (see the middle figure for an example); those coming from the vortex return to it and those starting sufficiently far from the vortex go to infinity (cf. right figure).

and to compute conjugate points in normal and abnormal cases. Second, we observe that the dynamics can be integrated using a generalization of the methods used for 2d-integrable mechanical systems as a step to compute action-angle variables. This leads to introduce in our frame, an extended potential. The application is to analyze the geodesics using an extension of the Morse-Reeb classification[6].

These techniques are used to study three case studies which are the core of the article. The first one is to recover in a neat geometric context the seminal results in the historical example. The second study is related to celestial and space mechanics and is analyzed by homotopy starting from the weak current to strong current, and deforming metrics on two-spheres of revolution. The interest of this case is to prove that in general the cut locus splits into two branches. The first branch being formed by the standard Riemann-Finsler case, thanks to continuity of the value function. But a second branch occurs in the strong current domain and is associated to the semicubical singularity of the abnormal direction, with neighboring self-intersecting normal extremals. Cut point occurs as intersection of abnormal and normal minimizing arcs but with distinct minimal times. This phenomenon, already observed in the historical example, is shown to be related to non-continuity property of the value function and is interpreted in a general frame of singularity theory. The third case study concerns a generalization of the navigation of a passive tracer, to generate complex dynamics, in particular with several equators and separatrices. All these cases can be glued to provide a serie of case studies, using combination of mathematical and numerical computations, with nice 2d-representations and using adapted softwares.

This article paves the road to many further studies. First of all, the techniques extend to general Zermelo

navigation problems on surfaces of revolution, since the assumption about parallel current can be relaxed, although the Morse-Reeb classification is more complex. Second, the results about the semicubical singularity of the abnormal geodesic when meeting the boundary of the strong domain can be generalized to generic Zermelo navigation problems, since the integrability of the geodesic flow is not an issue[15]. Finally, a new branch of the cut locus is detected in the problem in relation with non-continuity of the value function. A mathematical challenge is to make a complete description of the cut points, at least for 2d-Zermelo navigation problems and a first step towards is a generalization to planar time minimal control problems.

Finally, this article is a step towards the aim of an automatic computations of planar time minimal syntheses, in relation with classification of solutions of dynamical systems. Note in particular the relation between Reeb's graphs[6] and the generalized Morse-Reeb classification in our study.

References

- [1] V. I. Arnold and B. A. Khesin, *Topological Methods in Hydrodynamics*. Vol **125** of Applied Mathematical Sciences, Springer-Verlag New York, 1998, 376 pages.
- [2] V. I. Arnold, *Mathematical methods of classical mechanics*. Translated from the Russian by K. Vogtmann and A. Weinstein. Second edition. Graduate Texts in Mathematics, **60**. Springer-Verlag, New York, 1989, 508 pages.
- [3] V. I. Arnold, *The theory of singularities and its applications, Lezioni Fermiane*. Fermi Lectures, Accademia Nazionale dei Lincei, Rome, Scuola Normale Superiore, Pisa, 1991, 73 pages.
- [4] C. Balsa, O. Cots, J. Gergaud and B. Wembe, *Minimum energy control of passive tracers advection in point vortices flow*. In: Gonçalves J.A., Braz-César M., Coelho J.P. (eds) CONTROLLO 2020. Lecture Notes in Electrical Engineering, vol 695. Springer, Cham.
- [5] D. Bao, S. S. Chern and Z. Shen, *An Introduction to Riemann-Finsler Geometry*. Vol 200 of Graduate Texts in Mathematics, Springer-Verlag New York, 2000, 435 pages.
- [6] A. V. Bolsinov and A. T. Fomenko, *Integrable Hamiltonian Systems, Geometry, Topology, Classification*. Chapman and Hall/CRC, London, 2004, 724 pages.
- [7] B. Bonnard and J.-B. Caillau, *Geodesic flow of the averaged controlled Kepler equation*. Forum Math. **21** (2009), no. 5, pp. 797–814.
- [8] B. Bonnard, J.-B. Caillau and G. Janin, *Conjugate-cut loci and injectivity domains on two-spheres of revolution*. ESAIM: COCV **19** (2013), no. 2, pp. 533–554.
- [9] B. Bonnard, J.-B. Caillau, R. Sinclair and M. Tanaka, *Conjugate and cut loci of a two-sphere of revolution with application to optimal control*. Ann. Inst. H. Poincaré Anal. Non Linéaire **26** (2009), no. 4, pp. 1081–1098.
- [10] B. Bonnard and M. Chyba, *Singular trajectories and their role in control theory*. Vol **40** of *Mathematics & Applications*, Springer-Verlag, Berlin (2003), 357 pages.
- [11] B. Bonnard, O. Cots and N. Shcherbakova, *Riemannian metrics on 2D-manifolds related to the Euler-Poinsot rigid body motion*. ESAIM: COCV **20** (2014), no. 3 pp. 864–893.
- [12] B. Bonnard, O. Cots, J. Gergaud and B. Wembe, *Abnormal Geodesics in 2D-Zermelo Navigation Problems in the Case of Revolution and the Fan Shape of the Small Time Balls*. Systems & Control Letters **161** (2022) no 105140.
- [13] B. Bonnard, O. Cots and B. Wembe, *A Zermelo Navigation Problem with a Vortex Singularity*. ESAIM Control Optim. Calc. Var., **27** (2021), no. S10, 37 pages.
- [14] B. Bonnard and I. Kupka, *Théorie des singularités de l'application entrée/sortie et optimalité des trajectoires singulières dans le problème du temps minimal*. Forum Math., **5** (1993), no. 2, pp. 111–159.

- [15] B. Bonnard, J. Rouot and B. Wembe, *Accessibility properties of abnormal geodesics in optimal control illustrated by two case studies*, Mathematical Control and Related Fields, (2022) <https://doi.org/10.3934/mcrf.2022052>.
- [16] A. E. Bryson and Y. C. Ho, *Applied optimal control*. Hemisphere Publishing, New-York, 1975, 481 pages.
- [17] J.-B. Caillau, O. Cots and J. Gergaud, *Differential continuation for regular optimal control problems*. Optimization Methods and Software, **27** (2011), no. 2, pp. 177–196.
- [18] C. Carathéodory, *Calculus of Variations and Partial Differential Equations of the First Order, Part 1, Part 2*. Holden-Day, San Francisco, California, 1965-1967; Reprint: 2nd AMS printing, AMS Chelsea Publishing, Providence, RI, USA (2001), 412 pages.
- [19] M. P. Do Carmo, *Riemannian geometry*. Birkhäuser, Mathematics: Theory & applications, 2nd edn 1988, 300 pages.
- [20] G. Godbillon, *Feuilletages, études géométriques*, Progr. Math. 98, Birkhäuser, Boston, 1991, 475 pages.
- [21] W. B. Gordon, *A minimizing property of Keplerian orbits*. AMS, **99** (1977), no 5, pp. 962– 971.
- [22] V. Grines, E. Gurevich, O. Pochinka and D. Malyshev, *On topological classification of Morse-Smale diffeomorphisms on the sphere S^n , ($n > 3$)*. Nonlinearity **33** (2020), no. 12, pp. 7088–7113.
- [23] R. Hama, J. Kasemsuwan and S. V. Sabau, *The cut locus of a Randers rotational 2-sphere of revolution*, Publ. Math. Debrecen, **93** (2018), no 3-4, pp. 387–412.
- [24] J. Itoh and K. Kiyohara, *The cut loci and the conjugate loci on ellipsoids*. Manuscripta math., **114** (2004), no. 2, pp. 247–264.
- [25] I. Kupka. *Abnormal extremals*, Preprint (1992).
- [26] R. K. Meyer and G. R. Hall, *Introduction to Hamiltonian dynamical systems and the N-body problem*. Applied Mathematical Sciences, Springer-Verlag, New York, **90** (1992), 292 pages.
- [27] H. Poincaré, *Sur les lignes géodésiques des surfaces convexes. (French) [On the geodesic lines of convex surfaces]*. Trans. Amer. Math. Soc. **6** (1905), no. 3, pp. 237–274.
- [28] L. S. Pontryagin, V. G. Boltyanskiĭ, R. V. Gamkrelidze and E. F. Mishchenko, *The Mathematical Theory of Optimal Processes*. Translated from the Russian by K. N. Trirogoff, edited by L. W. Neustadt, Interscience Publishers John Wiley & Sons, Inc., New York-London, (1962), 360 pages.
- [29] C. L. Siegel and J. K. Moser, *Lectures on celestial mechanics*. Translation by Charles I. Kalme. Die Grundlehren der mathematischen Wissenschaften, Band **187**. Springer-Verlag, New York-Heidelberg (1971), 290 pages.
- [30] H. J. Sussmann, *The Structure of Time-Optimal Trajectories for Single-Input Systems in the Plane: The C^∞ Nonsingular Case*. SIAM J. Control Optim. **25** (1987), no. 2, pp. 433–465.
- [31] H. J. Sussmann, *Regular Synthesis for Time-Optimal Control of Single-Input Real Analytic Systems in the Plane*. SIAM J. Control Optim. **25** (1987), no. 5, pp. 1145–1162.
- [32] R. J. Walker, *Algebraic curves*, Springer-Verlag, New York, 1978, 201 pages.
- [33] B. Wembe, *Méthodes Géométriques et Numériques en Contrôle Optimal et Problèmes de Zermelo sur les Surfaces de Révolution - Applications*, Phd thesis, Université Toulouse Paul Sabatier, Toulouse, 2021.
- [34] E. Zermelo, *Über das Navigationsproblem bei ruhender oder veränderlicher wind-vertelung*. Z. Angew. Math. Mech., **11** (1931), no. 2, pp. 114–124.